

# Axis Tour: Word Tour Determines the Order of Axes in ICA-transformed Embeddings

Hiroaki Yamagiwa<sup>1</sup> Yusuke Takase<sup>1</sup> Hidetoshi Shimodaira<sup>1,2</sup>  
<sup>1</sup>Kyoto University <sup>2</sup>RIKEN AIP  
{hiroaki.yamagiwa, y.takase}@sys.i.kyoto-u.ac.jp,  
shimo@i.kyoto-u.ac.jp

## Abstract

Word embedding is one of the most important components in natural language processing, but interpreting high-dimensional embeddings remains a challenging problem. To address this problem, Independent Component Analysis (ICA) is identified as an effective solution. ICA-transformed word embeddings reveal interpretable semantic axes; however, the order of these axes is arbitrary. In this study, we focus on this property and propose a novel method, Axis Tour, which optimizes the order of the axes. Inspired by Word Tour, a one-dimensional word embedding method, we aim to improve the clarity of the word embedding space by maximizing the semantic continuity of the axes. Furthermore, we show through experiments on downstream tasks that Axis Tour yields better or comparable low-dimensional embeddings compared to both PCA and ICA.

## 1 Introduction

Embedding is an important tool in natural language processing, but interpreting high-dimensional embeddings is challenging. To address this, Independent Component Analysis (ICA) (Hyvärinen and Oja, 2000) offers an effective solution (Mareček et al., 2020; Musil and Mareček, 2024; Yamagiwa et al., 2023). ICA-transformed embeddings reveal interpretable semantic axes; however, the order of these axes is arbitrary (Hyvärinen et al., 2001b). In this study, inspired by a one-dimensional word embedding method, Word Tour (Sato, 2022), which leverages the Traveling Salesman Problem (TSP), we aim to improve the clarity of the word embedding space by maximizing the semantic continuity of the axes.

Figure 1 shows two sets of two-dimensional projections of word embeddings: one is ordered by Axis Tour (our proposal), and the other is sorted in descending order of skewness (Skewness Sort). In Axis Tour, the top words of the axes are positioned farther from the center, with the meanings of the

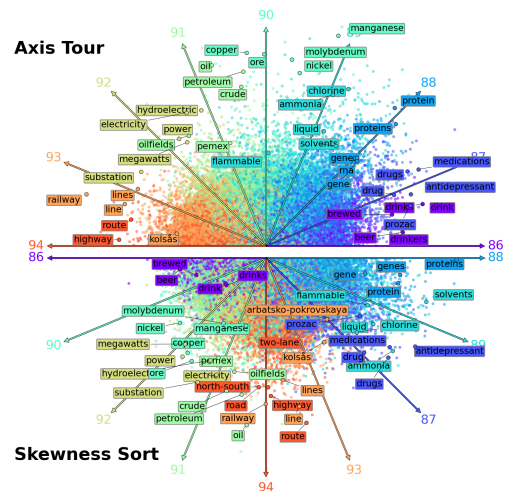


Figure 1: Scatterplots of normalized ICA-transformed word embeddings whose axes are ordered by Axis Tour and Skewness Sort. In the upper part, Axis Tour is applied to 300-dimensional GloVe, with nine consecutive axes arranged counterclockwise. In the lower part, these nine axes are rearranged clockwise in descending order of skewness. The embeddings are projected onto two dimensions along these axes. The top five embeddings on each axis are labeled by their words. Each word is assigned the color of the axis with the highest value. In both cases, words that cross the horizontal axes are not displayed. Refer to Appendix A for more details.

axes changing continuously. Conversely, in Skewness Sort, the top words are closer to the center, and the axes with different meanings are placed adjacently. In fact, the average distance from the origin to the top words in Fig. 1 is 0.76 in Axis Tour, compared to 0.61 in Skewness Sort.

We also assume that the consecutive axes in the Axis Tour embeddings can be considered a subspace with axes that have similar meanings. Based on this idea, we project each subspace onto a single dimension for dimensionality reduction. We show through experiments that Axis Tour yields better or comparable low-dimensional embeddings compared to both PCA and ICA.

## 2 Related work

Some studies transform embeddings by rotation (Park et al., 2017) from Factor Analysis (Crawford and Ferguson, 1970; Browne, 2001) or Principal Component Analysis (PCA) (Musil, 2019). Independent Component Analysis (ICA) (Hyvärinen and Oja, 2000) has gained attention for its ability to reveal interpretable semantic axes in the transformed embeddings (Mareček et al., 2020; Musil and Mareček, 2024; Yamagiwa et al., 2023).

Research on interpreting embeddings by focusing on axes representing opposing concepts (e.g., *cold* vs. *hot*, *soft* vs. *hard*) is also actively pursued. Approaches such as SemAxis (An et al., 2018), POLAR (Mathew et al., 2020), and FrameAxis (Kwak et al., 2021) deal with static embeddings, while Bi-Imp (Senel et al., 2022) and SensePOLAR (Engler et al., 2022) deal with dynamic embeddings. In particular, Section 5.3 provides a comparison of the Axis Tour embeddings and those from POLAR.

Relevant to our study is Topographic ICA (TICA) (Kohonen, 2001; Hyvärinen et al., 2001a). TICA relaxes the assumption of statistical independence and assumes higher-order correlations between adjacent axes. It then estimates the order of the axes. Unlike TICA, Axis Tour is applied to ordinary ICA-transformed embeddings and uses the embeddings themselves to measure axis similarity. For more details on TICA, refer to Appendix F.

## 3 Background

The pre-trained word embedding matrix is given by  $\mathbf{X} = [\mathbf{x}_1, \dots, \mathbf{x}_n]^\top \in \mathbb{R}^{n \times d}$ , where  $\mathbf{X}$  is *centered* (i.e., the mean of each column is zero). Here,  $\mathbf{x}_i \in \mathbb{R}^d$  represents the word embedding of the  $i$ -th word.

### 3.1 ICA-transformed word embeddings

ICA (Hyvärinen and Oja, 2000) finds the transformation matrix  $\mathbf{B} \in \mathbb{R}^{d \times d}$  such that the columns of the matrix  $\mathbf{S} \in \mathbb{R}^{n \times d}$ , represented by the following equation, are as independent as possible:

$$\mathbf{S} = \mathbf{XB}, \quad (1)$$

where  $\mathbf{S}$  is *whitened* (i.e., the variances of the columns are 1 and their correlations are all 0). The columns of  $\mathbf{S}$  are called independent components<sup>1</sup>. While  $\mathbf{S}$  has interpretable semantic axes (Mareček et al., 2020; Musil and Mareček, 2024; Yamagiwa

<sup>1</sup>Unless otherwise noted, flip the sign of each axis as needed so that the skewness is positive.

et al., 2023), the order of these axes are arbitrary (Hyvärinen et al., 2001b).

### 3.2 Word Tour

Let  $\mathcal{P}([n])$  be the set of all permutations of  $[n]$ , where  $[n] = \{1, \dots, n\}$ . Word Tour (Sato, 2022) is a one-dimensional word embedding method that solves the following Traveling Salesman Problem (TSP):

$$\min_{\tau \in \mathcal{P}([n])} \|\mathbf{x}_{\tau_1} - \mathbf{x}_{\tau_n}\| + \sum_{i=1}^{n-1} \|\mathbf{x}_{\tau_i} - \mathbf{x}_{\tau_{i+1}}\|. \quad (2)$$

The resulting one-dimensional embeddings have similar meanings when they are close in order.

## 4 Axis Tour

This section explains Axis Tour and the dimensionality reduction method using Axis Tour. As mentioned in Section 3.2,  $[d] = \{1, \dots, d\}$  and  $\mathcal{P}([d])$  is the set of all permutations of  $[d]$ .

### 4.1 Definition of axis embedding

We define *axis embedding* for use in Word Tour. The embedding represents the meaning of the axis of the ICA-transformed embeddings  $\mathbf{S}$ .

In preparation, we define the *normalized ICA-transformed embeddings*  $\hat{\mathbf{S}} \in \mathbb{R}^{n \times d}$  as the normalization of the embeddings  $\mathbf{S}$ , where the row vectors are given by  $\hat{\mathbf{s}}_i = \mathbf{s}_i / \|\mathbf{s}_i\|$ . Here, the  $i$ -th word embeddings of  $\mathbf{S}$  and  $\hat{\mathbf{S}}$  are denoted by  $\mathbf{s}_i$  and  $\hat{\mathbf{s}}_i \in \mathbb{R}^d$ , respectively. We compare the elements of the  $\ell$ -th axis of  $\hat{\mathbf{S}}$  and denote the index set of words corresponding to the top  $k$  elements as  $\text{Top}_k^\ell$ . We then define the  $\ell$ -th axis embedding  $\mathbf{v}_\ell$  for  $\mathbf{S}$  as follows:

$$\mathbf{v}_\ell := \frac{1}{k} \sum_{i \in \text{Top}_k^\ell} \hat{\mathbf{s}}_i \in \mathbb{R}^d. \quad (3)$$

As we saw in Fig. 1, since the meaning of an axis can be interpreted from the top words,  $\mathbf{v}_\ell$  can be considered the embedding that represents the meaning of the  $\ell$ -th axis of  $\mathbf{S}$ .

### 4.2 Determining the order of axes

Axis Tour is a method that uses  $\mathbf{v}_\ell$  in (3) to perform Word Tour and determines the order of axes in ICA-transformed word embeddings. In Axis Tour, the cost between the axis embeddings  $\mathbf{v}_\ell$  and  $\mathbf{v}_m$  for the TSP is defined by  $1 - \cos(\mathbf{v}_\ell, \mathbf{v}_m)$  instead of  $\|\mathbf{v}_\ell - \mathbf{v}_m\|$ . This approach then maximizes the sum of cosine similarities between adjacent axis

23	24	25	26	27	28	29	30	31
serb	russian	czech	germany	france	canada	australia	wiltshire	liga
bosnian	russia	prague	german	french	canadian	australian	shrewsbury	relegated
croatia	moscow	poland	berlin	le	ontario	queensland	lincolnshire	fc
croatian	sergei	polish	von	paris	quebec	brisbane	peterborough	f.c.
serbian	aleksandr	warsaw	cologne	du	saskatchewan	perth	croydon	serie
101	102	103	104	105	106	107	108	109
pay	land	laws	court	lawsuits	charges	camp	corpses	remain
fees	property	regulations	judge	lawsuit	alleged	prison	corpse	remained
payments	lands	enacted	appellate	litigation	prosecutors	buchenwald	exhumed	stayed
payment	estate	law	appeals	suits	indicted	camps	dismembered	stubbornly
paid	bergisches	provisions	supreme	suit	convicted	inmates	bodies	stays
237	238	239	240	241	242	243	244	245
award	film	superhero	album	piano	paintings	manuscript	language	name
awards	films	marvel	albums	violin	painting	biographies	languages	names
awarded	movie	spin-off	band	cello	art	pages	pashto	surname
prize	starring	superheroes	self-titled	percussion	sculpture	book	colloquial	phrase
emmy	directed	characters	ep	orchestral	watercolor	handwritten	dialect	misspelling

Table 1: Semantic continuity of axes by Axis Tour for normalized ICA-transformed embeddings. We apply Axis Tour to 300-dimensional GloVe and show the top five words for each axis. See Appendix E.1 for all axes results.

embeddings. Therefore, the problem is formulated as follows<sup>2</sup>:

$$\max_{\tau \in \mathcal{P}([d])} \cos(\mathbf{v}_{\tau_1}, \mathbf{v}_{\tau_d}) + \sum_{\ell=1}^{d-1} \cos(\mathbf{v}_{\tau_\ell}, \mathbf{v}_{\tau_{\ell+1}}). \quad (4)$$

The sum of cosine similarities between adjacent axis embeddings can be considered as a metric of the semantic continuity of the axes. Thus, Axis Tour determines the order of the axes by maximizing this metric.

### 4.3 Dimensionality reduction

Let  $\mathbf{T} = [\mathbf{t}_1, \dots, \mathbf{t}_n]^\top \in \mathbb{R}^{n \times d}$  be the matrix  $\mathbf{S}$  with Axis Tour applied, where the optimal  $\tau$  is applied to the columns of  $\mathbf{S}$  to produce  $\mathbf{T}$ . We consider reducing the dimensions from  $d$  to  $p$  ( $\leq d$ ) by merging the consecutive axes of  $\mathbf{T}$ . In preparation, we divide  $[d]$  into  $p$  equal-length intervals<sup>3</sup> and define the index set for the  $r$ -th interval as  $I_r := \{a_r, \dots, b_r\}$  ( $a_r, b_r \in [d], a_r \leq b_r$ ). Let  $\gamma_\ell \in \mathbb{R}_{\geq 0}$  be the skewness<sup>4</sup> of the  $\ell$ -th axis of  $\mathbf{T}$ .

First, we consider reducing the dimensionality of  $\mathbf{T}$  along  $I_r$ ,  $r = 1, \dots, p$ . To do this, we define a unit vector  $\mathbf{f}_r := (f_r^{(\ell)})_{\ell=1}^d \in \mathbb{R}_{\geq 0}^d$  for each  $I_r$  as follows:

$$f_r^{(\ell)} = \begin{cases} \gamma_\ell^\alpha / \sqrt{\sum_{m=a_r}^{b_r} \gamma_m^{2\alpha}} & \text{for } \ell \in I_r \\ 0 & \text{otherwise,} \end{cases} \quad (5)$$

<sup>2</sup>Note that due to the cyclic nature of  $\tau$ , we set  $\tau_1$  such that  $\cos(\mathbf{v}_{\tau_1}, \mathbf{v}_{\tau_d})$  is the smallest of the cosine similarities.

<sup>3</sup>The first  $d\%p$  intervals are  $\lfloor d/p \rfloor + 1$  in length, and the rest are  $\lfloor d/p \rfloor$  in length, where  $\lfloor \cdot \rfloor$  is the floor function.

<sup>4</sup>Since the skewness of the axis of  $\mathbf{S}$  is positive,  $\gamma_\ell \geq 0$ .

where  $\alpha \in \mathbb{R}_{\geq 0}$ . Then  $\mathbf{T}\mathbf{f}_r \in \mathbb{R}^n$  can be considered as a projection of the subspace spanned by the axes of  $\mathbf{T}$  corresponding to  $I_r$  onto a one-dimensional space. Fig. 7 in Appendix B shows the projection for three consecutive axes.

Next, we define the matrix  $\mathbf{F} := [\mathbf{f}_1, \dots, \mathbf{f}_p] \in \mathbb{R}^{d \times p}$ . Then  $\mathbf{TF} \in \mathbb{R}^{n \times p}$  represents the concatenated projections, that is, a dimensionality reduction of the  $d$ -dimensional embeddings  $\mathbf{T}$  to  $p$  dimensions. For more details, refer to Appendix B.

## 5 Experiments

Similar to the Word Tour experiments, we used 300-dimensional GloVe (Pennington et al., 2014) with  $n = 400,000$ , and the LKH solver<sup>5</sup> (Helsgaun, 2018) for the optimization of the TSP.

For ICA, we used FastICA (Hyvärinen, 1999) from scikit-learn (Pedregosa et al., 2011), setting the iterations to 10,000 and the tolerance to  $10^{-10}$ , consistent with Yamagiwa et al. (2023). We computed the axis embeddings<sup>6</sup>  $\mathbf{v}_\ell$  in (3) with  $k = 100$ . For baselines, we used whitened PCA-transformed embeddings<sup>7</sup>, along with two types of whitened ICA-transformed embeddings<sup>8</sup>: **Random Order**, which randomly flips the sign of the axes in  $\mathbf{S}$  and randomizes the order of the axes, and **Skewness Sort**, which sorts the axes of  $\mathbf{S}$  in descending order of skewness. See Appendix E for additional

<sup>5</sup>The LKH solver is an implementation of Lin-Kernighan algorithm (Lin and Kernighan, 1973; Helsgaun, 2000).

<sup>6</sup>See Appendix E.3 for a discussion of the choice of  $k$ .

<sup>7</sup>Whitened ICA-transformed embeddings are obtained by applying an orthogonal matrix to these embeddings.

<sup>8</sup>See Appendix F for comparisons of Axis Tour and TICA.

experiments, including those of other embeddings.

### 5.1 Qualitative observation of semantic continuity in axis order

Table 1 presents an illustrative example of consecutive axes of the Axis Tour embeddings, where the three rows correspond to the meanings of *countries*, *law*, and *art*, respectively. We observe that the meanings of the axes change continuously. For instance, in the top row, the axis meaning shifts from *Eastern Europe* to *Germany* and *France*, followed by *Canada* (which shares a connection with France), then to *Australia* (English-speaking regions), *the regions in England*, and finally to *soccer* (a popular sport in England), demonstrating geographic and cultural continuity.

### 5.2 Quantitative evaluation of semantic continuity in axis order

This section quantitatively evaluates the semantic continuity of the axes in Axis Tour embeddings.

#### 5.2.1 Evaluation by cosine similarity

First, we evaluate the two orderings of axes shown in Fig. 1. The semantic continuity of these axes is assessed by calculating the average cosine similarity between adjacent axis embeddings. For Axis Tour, the average cosine similarity is 0.269, but it decreases to 0.185 when these axes are rearranged by skewness, confirming the higher semantic continuity of the axes in Axis Tour.

Next, we consider the whole  $d (= 300)$  consecutive axes. Figure 2 shows the histograms of  $\cos(\mathbf{v}_\ell, \mathbf{v}_{\ell+1})$  for Axis Tour and the baselines. In Axis Tour, the values of  $\cos(\mathbf{v}_\ell, \mathbf{v}_{\ell+1})$  are consistently higher, while this trend is not observed in the other baselines. The average cosine similarity is 0.244 for Axis Tour, while it is only 0.017 for Skewness Sort. This result is consistent with the formulation in (4).

#### 5.2.2 Evaluation by GPT models

We also evaluate the semantic continuity of axes for Axis Tour and Skewness Sort using the OpenAI API. By focusing on the common axes in each embedding, we ask the model to determine, based on the top 10 words, whether the next axis of Axis Tour or that of Skewness Sort is more semantically related. The number of queries corresponds to  $d (= 300)$ , and we use four GPT models: GPT-3.5 Turbo, GPT-4 Turbo, GPT-4o, and GPT-4o mini (see Appendix G for model versions and prompts).

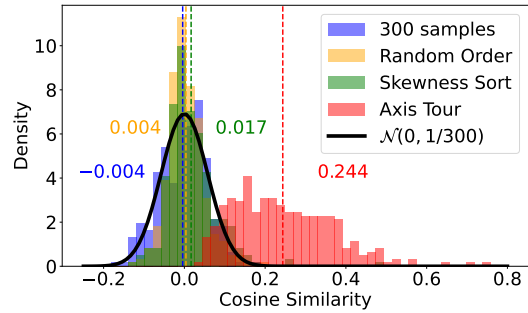


Figure 2: Histogram of  $\cos(\mathbf{v}_\ell, \mathbf{v}_{\ell+1})$ . As an additional baseline, we sampled 300 random words from the Random Order embeddings and arranged them in random order. The dashed lines represent the average similarity for each method. The distribution for Axis Tour shifts towards a more positive mean, while the others roughly follow a normal distribution with means close to 0. For more details, refer to Appendix C.

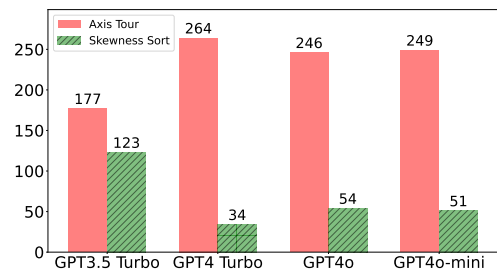


Figure 3: Comparison of the number of related axes in the GPT models. In each model, Axis Tour exhibits a greater number of related axes than Skewness Sort.

As shown in Fig. 3, Axis Tour has a greater number of related axes compared to Skewness Sort for each model, implying more continuous changes in axis meanings. The smallest difference was observed with GPT-3.5 Turbo, the least performant model. For the other models (i.e., the GPT-4 models), the difference was at least four times larger.

### 5.3 Dimensionality reduction: analogy, word similarity, and categorization tasks

Using Word Embedding Benchmark (Jastrzebski et al., 2017)<sup>9</sup>, we evaluate the performance of dimensionality reduction in analogy, word similarity, and categorization tasks. PCA selects the axes in descending order of eigenvalue. Random Order and Skewness Sort select the axes sequentially from first to last. Axis Tour adopts the dimensionality reduction<sup>10</sup> in Section 4.3 with  $\alpha = 1/3$ .

We consider the original GloVe embeddings  $\mathbf{X}$

<sup>9</sup><https://github.com/kudkudak/word-embeddings-benchmarks>.

<sup>10</sup>Fig. 8 in Appendix E.2 shows the results for different  $\alpha$ .

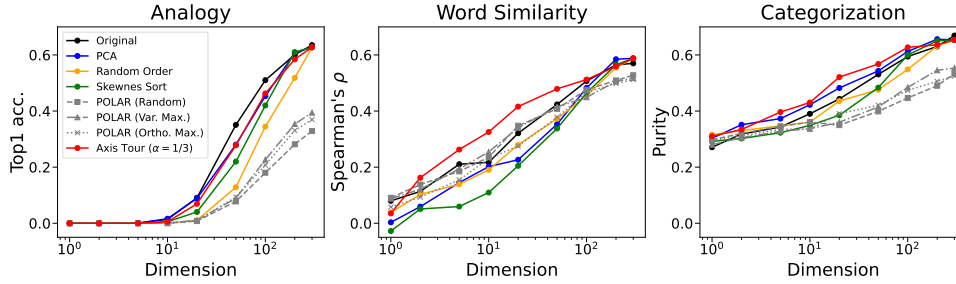


Figure 4: The performance of dimensionality reduction for embeddings. Each value represents the average of 30 analogy tasks, 8 word similarity tasks, or 6 categorization tasks. See Appendix D for detailed experimental results.

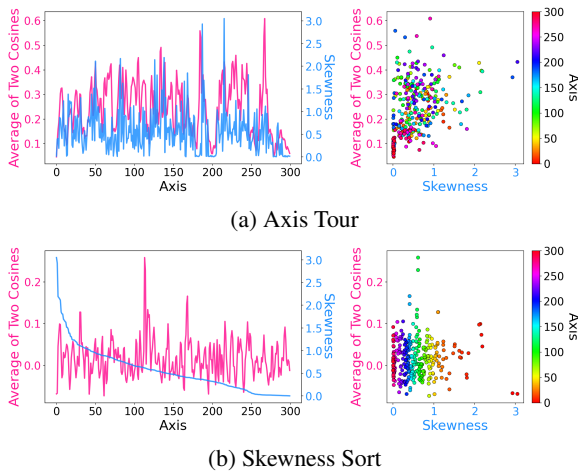


Figure 5: Relationship between the skewness  $\gamma_\ell$  and the average of two consecutive cosines  $(\cos(\mathbf{v}_{\ell-1}, \mathbf{v}_\ell) + \cos(\mathbf{v}_\ell, \mathbf{v}_{\ell+1}))/2$  for all the axes  $\ell = 1, \dots, d$  in (a) Axis Tour and (b) Skewness Sort. The left plot shows the skewness and the average of two cosines on both  $y$ -axes, while the right plot shows the scatter plot of these values. Spearman’s rank correlation is 0.43 for Axis Tour, while it is 0.04 for Skewness Sort.

as well as the embeddings obtained by applying POLAR to  $\mathbf{X}$ . POLAR is a method that uses pairs of words with opposite meanings and finds the axes where these words are positioned at the opposite ends. There are three methods for selecting the axes: Random Selection, Variance Maximization, and Orthogonality Maximization. We used the publicly available code for our experiments. For both the original and POLAR-applied embeddings, axes were selected sequentially from first to last.

Figure 4 shows that the dimensionality reduction with the ordering in Axis Tour is better than or comparable to the baselines for most dimensionalities in each task. This result suggests that Axis Tour efficiently merges axes with similar meanings. For more details, refer to Appendix D.

## 6 Discussion

We confirmed through both qualitative and quantitative experiments that the axis order determined by Axis Tour exhibits high semantic continuity, and its effectiveness was also validated in the downstream task of dimensionality reduction.

There are two advantages to ordering the axes of ICA-transformed embeddings using Axis Tour. First, as shown in Fig. 1, when projecting the embedding space, the scatterplot becomes easier to interpret and more visually accessible because higher-ranking words on each axis are farther from the origin. Second, although the Axis Tour embeddings  $\mathbf{T}$  are the same size as the ICA-transformed embeddings  $\mathbf{S}$ , the axis order in Axis Tour preserves information about the similarities between the axes.

An interesting relationship between semantic continuity and skewness is shown in Fig. 5, where the semantic continuity of axis  $\ell$  is measured by the average of two cosines. In Axis Tour, there is a high correlation between skewness and semantic continuity, while in Skewness Sort, they are almost uncorrelated. A large skewness indicates that an axis has a distinctive meaning, and in Axis Tour, this seems to contribute to semantic continuity.

## 7 Conclusion

In this study, we proposed a novel method, Axis Tour, which optimizes the order of axes in ICA-transformed word embeddings. We focused on the fact that the word embeddings reveal interpretable semantic axes while the order of these axes is arbitrary. Axis Tour aims to improve the clarity of the word embedding space by maximizing the semantic continuity of the axes. Additionally, we demonstrated through experiments on downstream tasks that Axis Tour yields better or comparable low-dimensional embeddings compared to both PCA and ICA.

## Limitations

- While the dimension reduction experiments showed the improvement of the downstream task performance for the Axis Tour embeddings, there are three aspects that could be further improved:
  1. Dimension reduction is performed using the vector  $\mathbf{f}_r$ , but its definition (5) is empirical, and better vectors may be designed. In addition, nonlinear transformations beyond linear ones could be considered for dimension reduction. Details on the definition of  $\mathbf{f}_r$  can be found in Appendix B.
  2. The method in Section 4.3 simply divides  $[d]$  into  $p$  equal intervals to merge the axes. However, adaptively determining the division points could allow selecting more semantically coherent groups of axes.
  3. To construct optimal low-dimensional vectors using ICA-transformed embeddings, applying clustering methods such as  $K$ -means to axis embeddings may improve performance. In this case, the overall optimized axis order may not be determined as in Axis Tour, but performing Axis Tour within each cluster and then concatenating these could determine an axis order depending on the number of clusters.

However, this study focuses on a method for maximizing the semantic continuity of axes in ICA-transformed embeddings, leaving detailed investigation of the effective low-dimensional vector as future work.

- In Axis Tour, while adjacent axes may have similar meanings, axes with similar meanings may not be in close order. This is due to the fact that in Word Tour, high-dimensional embeddings result in one-dimensional embeddings, and the meanings of words are similar when the word order is close, but semantically similar words are not always embedded close to each other.
- As seen in Fig. 1, projecting multiple axes of ICA-transformed embeddings into two dimensions can effectively represent the shape of the embeddings. However, as the number of

axes increases, the angles between the axes become small, resulting in crowded axes. This can cause problems such as the top words of the axes being closer to the origin, which can be difficult to interpret.

- In Axis Tour, the dimension of the ICA-transformed embeddings corresponds to the number of cities in TSP. Therefore, as the dimension of the embeddings increases, the computation time for Axis Tour becomes longer. Note that for the 300-dimensional GloVe used in this study, the computation time for Axis Tour is about one second. For reference, Word Tour with  $n = 40,000$  is known to take several hours<sup>11</sup>.

## Ethics Statement

A potential risk of this method is that we interpret the meanings of the axes of the ICA-transformed embeddings by the top words of each axis. If the embeddings contain personal information, such as email addresses or phone numbers, and these are contained in the top words, this can be problematic. Therefore, in this study, URLs, email addresses, and phone numbers were anonymized to avoid revealing such information.

## Acknowledgements

We would like to thank Momose Oyama for the discussion and anonymous reviewers for their helpful advice. This study was partially supported by JSPS KAKENHI 22H05106, 23H03355, JST CREST JPMJCR21N3, JST SPRING JPMJSP2110.

## Code availability

Our code is available at <https://github.com/ymgw55/Axis-Tour>.

## References

- Abdulrahman Almuhareb and Massimo Poesio. 2005. [Concept learning and categorization from the web](#). *Proceedings of the Annual Meeting of the Cognitive Science Society*, 27.
- Jisun An, Haewoon Kwak, and Yong-Yeol Ahn. 2018. [Semaxis: A lightweight framework to characterize domain-specific word semantics beyond sentiment](#). In *Proceedings of the 56th Annual Meeting of the Association for Computational Linguistics, ACL 2018, Melbourne, Australia, July 15-20, 2018, Volume 1*:

<sup>11</sup><https://github.com/joisino/wordtour>.

- Long Papers*, pages 2450–2461. Association for Computational Linguistics.
- Marco Baroni, Stefan Evert, and Alessandro Lenci, editors. 2008. *Proceedings of the ESSLLI Workshop on Distributional Lexical Semantics: Bridging the Gap between Semantic Theory and Computational Simulations*. European Summer School in Logic, Language and Information (ESSLLI), Hamburg, Germany.
- Marco Baroni and Alessandro Lenci. 2011. [How we blessed distributional semantic evaluation](#). In *Proceedings of the GEMS 2011 Workshop on GEometrical Models of Natural Language Semantics, Edinburgh, UK, July 31, 2011*, pages 1–10. Association for Computational Linguistics.
- William F. Battig and William E. Montague. 1969. [Category norms of verbal items in 56 categories: A replication and extension of the connecticut category norms](#). *Journal of Experimental Psychology*, 80(3, Pt.2):1–46.
- Patrick Billingsley. 1995. *Probability and Measure, Third Edition*. Wiley Series in Probability and Statistics. Wiley.
- Michael W Browne. 2001. An overview of analytic rotation in exploratory factor analysis. *Multivariate behavioral research*, 36(1):111–150.
- Elia Bruni, Nam-Khanh Tran, and Marco Baroni. 2014. Multimodal distributional semantics. *Journal of Artificial Intelligence Research*, 49:1–47.
- Ciprian Chelba, Tomas Mikolov, Mike Schuster, Qi Ge, Thorsten Brants, Phillipp Koehn, and Tony Robinson. 2014. [One billion word benchmark for measuring progress in statistical language modeling](#). In *INTER-SPEECH 2014, 15th Annual Conference of the International Speech Communication Association, Singapore, September 14-18, 2014*, pages 2635–2639. ISCA.
- Charles B Crawford and George A Ferguson. 1970. A general rotation criterion and its use in orthogonal rotation. *Psychometrika*, 35(3):321–332.
- Hoagy Cunningham, Aidan Ewart, Logan Riggs, Robert Huben, and Lee Sharkey. 2023. [Sparse autoencoders find highly interpretable features in language models](#). *CoRR*, abs/2309.08600.
- Jacob Devlin, Ming-Wei Chang, Kenton Lee, and Kristina Toutanova. 2019. [BERT: pre-training of deep bidirectional transformers for language understanding](#). In *Proceedings of the 2019 Conference of the North American Chapter of the Association for Computational Linguistics: Human Language Technologies, NAACL-HLT 2019, Minneapolis, MN, USA, June 2-7, 2019, Volume 1 (Long and Short Papers)*, pages 4171–4186. Association for Computational Linguistics.
- Jan Engler, Sandipan Sikdar, Marlene Lutz, and Markus Strohmaier. 2022. [Sensepolar: Word sense aware interpretability for pre-trained contextual word embeddings](#). In *Findings of the Association for Computational Linguistics: EMNLP 2022, Abu Dhabi, United Arab Emirates, December 7-11, 2022*, pages 4607–4619. Association for Computational Linguistics.
- Lev Finkelstein, Evgeniy Gabrilovich, Yossi Matias, Ehud Rivlin, Zach Solan, Gadi Wolfman, and Eytan Ruppin. 2002. Placing search in context: The concept revisited. *ACM Transactions on information systems*, 20(1):116–131.
- Keld Helsgaun. 2000. [An effective implementation of the lin-kernighan traveling salesman heuristic](#). *Eur. J. Oper. Res.*, 126(1):106–130.
- Keld Helsgaun. 2018. [LKH \(Keld Helsgaun\)](#).
- Felix Hill, Roi Reichart, and Anna Korhonen. 2015. Simlex-999: Evaluating semantic models with (genuine) similarity estimation. *Computational Linguistics*, 41(4):665–695.
- Aapo Hyvarinen. 1999. [Fast and robust fixed-point algorithms for independent component analysis](#). *IEEE Trans. Neural Networks*, 10(3):626–634.
- Aapo Hyvarinen, Patrik O. Hoyer, and Mika Inki. 2001a. [Topographic independent component analysis](#). *Neural Comput.*, 13(7):1527–1558.
- Aapo Hyvarinen, Juha Karhunen, and Erkki Oja. 2001b. [Independent Component Analysis](#). Wiley.
- Aapo Hyvarinen and Erkki Oja. 2000. [Independent component analysis: algorithms and applications](#). *Neural Networks*, 13(4-5):411–430.
- Stanislaw Jastrzebski, Damian Lesniak, and Wojciech Marian Czarnecki. 2017. [How to evaluate word embeddings? on importance of data efficiency and simple supervised tasks](#). *CoRR*, abs/1702.02170.
- Teuvo Kohonen. 2001. [Self-Organizing Maps, Third Edition](#). Springer Series in Information Sciences. Springer.
- Haewoon Kwak, Jisun An, Elise Jing, and Yong-Yeol Ahn. 2021. [Frameaxis: characterizing microframe bias and intensity with word embedding](#). *PeerJ Comput. Sci.*, 7:e644.
- Shen Lin and Brian W. Kernighan. 1973. [An effective heuristic algorithm for the traveling-salesman problem](#). *Oper. Res.*, 21(2):498–516.
- Thang Luong, Richard Socher, and Christopher Manning. 2013. Better word representations with recursive neural networks for morphology. In *Proceedings of the Seventeenth Conference on Computational Natural Language Learning*, pages 104–113.

- David Mareček, Jindřich Libovický, Tomáš Musil, Rudolf Rosa, and Tomasz Limisiewicz. 2020. *Hidden in the Layers: Interpretation of Neural Networks for Natural Language Processing*, volume 20 of *Studies in Computational and Theoretical Linguistics*. Institute of Formal and Applied Linguistics, Prague, Czechia.
- Binny Mathew, Sandipan Sikdar, Florian Lemmerich, and Markus Strohmaier. 2020. *The POLAR framework: Polar opposites enable interpretability of pre-trained word embeddings*. In *WWW '20: The Web Conference 2020, Taipei, Taiwan, April 20-24, 2020*, pages 1548–1558. ACM / IW3C2.
- Tomáš Mikolov, Kai Chen, Greg Corrado, and Jeffrey Dean. 2013a. *Efficient estimation of word representations in vector space*. In *1st International Conference on Learning Representations, ICLR 2013, Scottsdale, Arizona, USA, May 2-4, 2013, Workshop Track Proceedings*.
- Tomáš Mikolov, Kai Chen, Greg Corrado, and Jeffrey Dean. 2013b. *Efficient estimation of word representations in vector space*. In *1st International Conference on Learning Representations, ICLR 2013, Scottsdale, Arizona, USA, May 2-4, 2013, Workshop Track Proceedings*.
- Tomáš Mikolov, Wen-tau Yih, and Geoffrey Zweig. 2013c. *Linguistic regularities in continuous space word representations*. In *Human Language Technologies: Conference of the North American Chapter of the Association of Computational Linguistics, Proceedings, June 9-14, 2013, Westin Peachtree Plaza Hotel, Atlanta, Georgia, USA*, pages 746–751. The Association for Computational Linguistics.
- Tomáš Musil. 2019. *Examining structure of word embeddings with PCA*. In *Text, Speech, and Dialogue - 22nd International Conference, TSD 2019, Ljubljana, Slovenia, September 11-13, 2019, Proceedings*, volume 11697 of *Lecture Notes in Computer Science*, pages 211–223. Springer.
- Tomáš Musil and David Mareček. 2024. *Exploring interpretability of independent components of word embeddings with automated word intruder test*. In *Proceedings of the 2024 Joint International Conference on Computational Linguistics, Language Resources and Evaluation (LREC-COLING 2024)*, pages 6922–6928, Torino, Italia. ELRA and ICCL.
- Sungjoon Park, JinYeong Bak, and Alice Oh. 2017. *Rotated word vector representations and their interpretability*. In *Proceedings of the 2017 Conference on Empirical Methods in Natural Language Processing, EMNLP 2017, Copenhagen, Denmark, September 9-11, 2017*, pages 401–411. Association for Computational Linguistics.
- Fabian Pedregosa, Gaël Varoquaux, Alexandre Gramfort, Vincent Michel, Bertrand Thirion, Olivier Grisel, Mathieu Blondel, Peter Prettenhofer, Ron Weiss, Vincent Dubourg, Jake VanderPlas, Alexandre Passos, David Cournapeau, Matthieu Brucher, Matthieu Perrot, and Edouard Duchesnay. 2011. *Scikit-learn: Machine learning in python*. *J. Mach. Learn. Res.*, 12:2825–2830.
- Jeffrey Pennington, Richard Socher, and Christopher D. Manning. 2014. *Glove: Global vectors for word representation*. In *Proceedings of the 2014 Conference on Empirical Methods in Natural Language Processing, EMNLP 2014, October 25-29, 2014, Doha, Qatar, A meeting of SIGDAT, a Special Interest Group of the ACL*, pages 1532–1543. ACL.
- Kira Radinsky, Eugene Agichtein, Evgeniy Gabrilovich, and Shaul Markovitch. 2011. *A word at a time: Computing word relatedness using temporal semantic analysis*. In *Proceedings of the 20th International Conference on World Wide Web*, page 337–346.
- Herbert Rubenstein and John B. Goodenough. 1965. *Contextual correlates of synonymy*. *Commun. ACM*, 8(10):627–633.
- Ryoma Sato. 2022. *Word tour: One-dimensional word embeddings via the traveling salesman problem*. In *Proceedings of the 2022 Conference of the North American Chapter of the Association for Computational Linguistics: Human Language Technologies, NAACL 2022, Seattle, WA, United States, July 10-15, 2022*, pages 2166–2172. Association for Computational Linguistics.
- Lütfi Kerem Senel, Furkan Sahinuç, Veysel Yücesoy, Hinrich Schütze, Tolga Çukur, and Aykut Koç. 2022. *Learning interpretable word embeddings via bidirectional alignment of dimensions with semantic concepts*. *Inf. Process. Manag.*, 59(3):102925.
- Robyn Speer. 2022. *rspeer/wordfreq: v3.0*.
- Thomas Wolf, Lysandre Debut, Victor Sanh, Julien Chaumond, Clement Delangue, Anthony Moi, Pierric Cistac, Tim Rault, Rémi Louf, Morgan Funtowicz, Joe Davison, Sam Shleifer, Patrick von Platen, Clara Ma, Yacine Jernite, Julien Plu, Canwen Xu, Teven Le Scao, Sylvain Gugger, Mariama Drame, Quentin Lhoest, and Alexander M. Rush. 2020. *Transformers: State-of-the-art natural language processing*. In *Proceedings of the 2020 Conference on Empirical Methods in Natural Language Processing: System Demonstrations, EMNLP 2020 - Demos, Online, November 16-20, 2020*, pages 38–45. Association for Computational Linguistics.
- Hiroaki Yamagiwa, Momose Oyama, and Hidetoshi Shimodaira. 2023. *Discovering universal geometry in embeddings with ICA*. In *Proceedings of the 2023 Conference on Empirical Methods in Natural Language Processing, EMNLP 2023, Singapore, December 6-10, 2023*, pages 4647–4675. Association for Computational Linguistics.



## A Details of scatterplots from two-dimensional projection

This section explains the two-dimensional projection method used for the scatterplots in Fig. 1. We then present similar scatterplots for the three examples in Table 1. Finally, we define the metrics used in Section 1 to evaluate the quality of the scatterplots.

### A.1 Scatterplot drawing method

We will explain the scatterplot drawing method using the Axis Tour embeddings.

First, we define a set of axis indices for projection. Let  $I := \{a, \dots, b\}$  ( $a, b \in [d], a < b$ ) be a consecutive interval of indices. The number of indices in  $I$  is  $|I| = b - a + 1$ . For example, in Fig. 1,  $a = 86$  and  $b = 94$ .

Next, we define a matrix by extracting the axes of  $\hat{\mathbf{T}}$  corresponding to  $I$ , where  $\hat{\mathbf{T}}$  is the matrix obtained by normalizing the matrix  $\mathbf{T}$ . We denote this extracted matrix as  $\hat{\mathbf{T}}_I \in \mathbb{R}^{n \times |I|}$ .

We consider the two-dimensional projection of  $\hat{\mathbf{T}}_I$ . For this projection, we define the matrix  $\mathbf{P}_I \in \mathbb{R}^{|I| \times 2}$  as follows<sup>12</sup>:

$$\mathbf{P}_I := \begin{bmatrix} \varphi_a^\top \\ \vdots \\ \varphi_b^\top \end{bmatrix} \in \mathbb{R}^{|I| \times 2}, \quad (6)$$

where

$$\varphi_\ell := (\cos \theta_\ell, \sin \theta_\ell)^\top \in \mathbb{R}^2, \quad (7)$$

where

$$\theta_\ell := \frac{(\ell - a)\pi}{b - a}. \quad (8)$$

Then we get the two-dimensional projection as  $\mathbf{Q}_I := \hat{\mathbf{T}}_I \mathbf{P}_I \in \mathbb{R}^{n \times 2}$ . In  $\mathbf{Q}_I$ , the  $\ell$ -th axis of  $\hat{\mathbf{T}}$  is projected along the direction of  $\varphi_\ell$ .

We denote the  $i$ -th word embedding of  $\mathbf{Q}_I$  by  $\mathbf{q}_i = (q_i^x, q_i^y)^\top \in \mathbb{R}^2$ . When we plot the scatterplot of  $\mathbf{Q}_I$ , we do not plot the  $i$ -th word embedding if  $q_i^y < 0$  for visual clarity, and show the top five words for each axis. The indices of these top words equal to the following index set  $\text{Show}_I$  defined with  $\text{Top}_k^\ell$  from section 4.1:

$$\text{Show}_I := \{i \in [n] \mid q_i^y \geq 0\} \cap \bigcup_{\ell \in I} \text{Top}_5^\ell. \quad (9)$$

<sup>12</sup> $I$  is a subinterval of  $d$  indices, and to prevent angles between  $\varphi_a$  and  $\varphi_b$  from becoming smaller,  $\theta_\ell$  is defined so that  $\theta_a = 0$  and  $\theta_b = \pi$ . If  $\theta_\ell = \frac{2(\ell - a)\pi}{b - a + 1}$ , as we see in Fig. 15 in Appendix C of Yamagiwa et al. (2023), the angle between  $\varphi_a$  and  $\varphi_b$  will be the same as between  $\varphi_\ell$  and  $\varphi_{\ell+1}$ .

Similarly, we can apply the same procedure to the Skewness Sort embeddings and obtain the two-dimensional scatterplot.

### A.2 Scatterplots of Table 1

Figure 6 shows the scatterplots of the two-dimensional projections for the axes of the Axis Tour embeddings in Table 1, using the procedure described in Appendix A.1. Similar to Fig. 1, it is evident that the top words of the axes of the Axis Tour embeddings are farther from the origin than those of the Skewness Sort, and the meanings of the adjacent axes change continuously.

### A.3 Evaluation metrics for scatterplots

In Section 1, we compared the quality of the scatterplots for Axis Tour and Skewness Sort by calculating the average distance of the top words from the origin. In this section, we first explain this metric and then, based on (4), define a new metric derived from the average of the cosine similarities between adjacent axis embeddings. We then compare these metrics for the scatterplots in Figs. 1 and 6. Similar to Appendix A.1, we use the Axis Tour embeddings to explain these metrics.

For the two-dimensional projection  $\mathbf{Q}_I$  of the Axis Tour embeddings, we define the average distance  $d_I$  of the top words from the origin, using the index set  $\text{Show}_I$  in (9), as follows:

$$d_I := \frac{1}{|\text{Show}_I|} \sum_{i \in \text{Show}_I} \|\mathbf{q}_i\| \quad (10)$$

A larger  $d_I$  indicates that the scatterplot more accurately reflects the spatial distribution of the original embeddings, since the top words are positioned far from the origin.

We also define the average cosine similarity between adjacent axis embeddings,  $c_I$ , for the interval  $I$  as follows:

$$c_I := \frac{1}{b - a} \sum_{\ell=a}^{b-1} \cos(\mathbf{v}_\ell, \mathbf{v}_{\ell+1}) \quad (11)$$

As we saw in (4), since Axis Tour optimizes the order of the axes to maximize the sum of the cosine similarities, the value of  $c_I$  reflects the semantic continuity of the axes in the scatterplot. It is important to note that  $I$  represents a subinterval of  $d$  indices, so we do not include the term of  $\cos(\mathbf{v}_a, \mathbf{v}_b)$  in (11).

Both  $d_I$  and  $c_I$  can also be calculated in a similar manner for Skewness Sort. Table 2 shows the

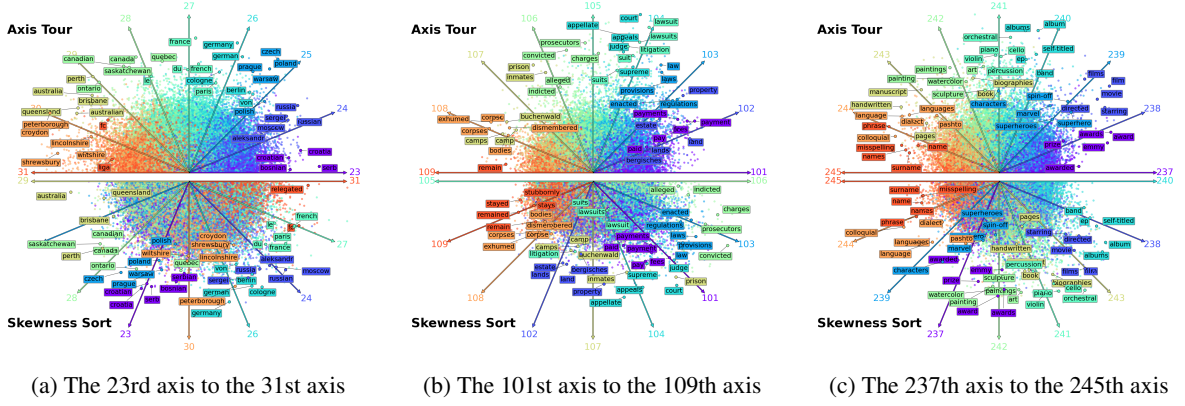


Figure 6: The scatterplots of the two-dimensional projections for the axes of the Axis Tour embeddings in Table 1. Similar to Fig. 1, we used the procedure described in Appendix A.1.

Fig.	Axis Tour		Skewness Sort	
	$d_I$	$c_I$	$d_I$	$c_I$
1	0.76	0.27	0.61	0.18
6a	0.69	0.28	0.61	0.10
6b	0.80	0.30	0.62	0.15
6c	0.86	0.38	0.76	0.23

Table 2: The values of  $d_I$  and  $c_I$  for Figs. 1 and 6.

values of  $d_I$  and  $c_I$  for Figs. 1 and 6. In these examples, Axis Tour shows higher values for both  $d_I$  and  $c_I$  compared to Skewness Sort, indicating better projection quality.

In addition to the results for several subintervals in Table 2, we also see the semantic continuity of all axes. If  $I = [d]$  in (11), we get  $c_I = c_{[d]}$  as follows

$$c_{[d]} = \frac{1}{d} \left\{ \cos(\mathbf{v}_1, \mathbf{v}_d) + \sum_{\ell=1}^{d-1} \cos(\mathbf{v}_\ell, \mathbf{v}_{\ell+1}) \right\} \quad (12)$$

where the term of  $\cos(\mathbf{v}_1, \mathbf{v}_d)$  is added according to (4). The value of  $c_{[d]}$  is equal to the average of the histogram in Fig. 2, so the value for Axis Tour is 0.244 and for Skewness Sort is 0.017, thus confirming the semantic continuity across all axes.

## B Dimensionality reduction

This section details and supplements Section 4.3.

### B.1 Definition of $\mathbf{f}_r$

Here we first discuss the definition of  $\mathbf{f}_r$  in terms of skewness and then explain the normalization.

#### B.1.1 Skewness as weight

In (3), a vector  $\mathbf{f}_r = (f_r^{(\ell)})_{\ell=1}^d \in \mathbb{R}_{\geq 0}^d$  for dimensionality reduction is defined by the skewness  $\gamma_\ell \in \mathbb{R}_{\geq 0}$  of the  $\ell$ -th axis of  $\mathbf{T}$ . In particular,  $f_r^{(\ell)}$ , which corresponds to the weight of the  $\ell$ -th axis in the projection, is proportional to  $\gamma_\ell^\alpha$  ( $\alpha \in \mathbb{R}_{\geq 0}$ ).

This is based on the assumption that the axis becomes more meaningful as the skewness increases<sup>13</sup>. Higher-order statistics such as skewness are known to be sensitive to outliers (Hyvärinen et al., 2001b), so we mitigate this effect by raising  $\gamma_\ell$  to the power of  $\alpha$ . Since skewness is a third-order moment, we treat  $\alpha = 1/3$  as the default value.  $\alpha = 0$  is a uniform weight, while  $\alpha = 1$  is the original  $\gamma_\ell$ . Next, we will explain why  $\mathbf{f}_r$  is normalized.

#### B.1.2 Reason for Normalizing $\mathbf{f}_r$

$\mathbf{f}_r$  is normalized (i.e.,  $\|\mathbf{f}_r\| = 1$ ) to equalize the scale of the one-dimensional projections for each subspace. Thus, when  $p = d$ ,  $\mathbf{TF} = \mathbf{T}$  holds.

For  $p = d$ ,  $I_r = \{r\}$ , and from (3),  $\mathbf{f}_r = (f_r^{(\ell)})_{\ell=1}^d$  satisfies:

$$f_r^{(\ell)} = \delta_{\ell r} = \begin{cases} 1 & \ell = r \\ 0 & \ell \neq r \end{cases}. \quad (13)$$

Here,  $\delta_{\ell r}$  is the Dirac delta function. From (13) the matrix  $\mathbf{F} = [\mathbf{f}_1, \dots, \mathbf{f}_d] \in \mathbb{R}^{d \times d}$  corresponds to the  $d$ -dimensional identity matrix  $\mathbf{I} \in \mathbb{R}^{d \times d}$ , so  $\mathbf{TF} = \mathbf{TI} = \mathbf{T}$ .

<sup>13</sup>While not specific to ICA-transformed embeddings, it is known from a study of sparse coding for language models that skewness correlates with interpretability (Cunningham et al., 2023).

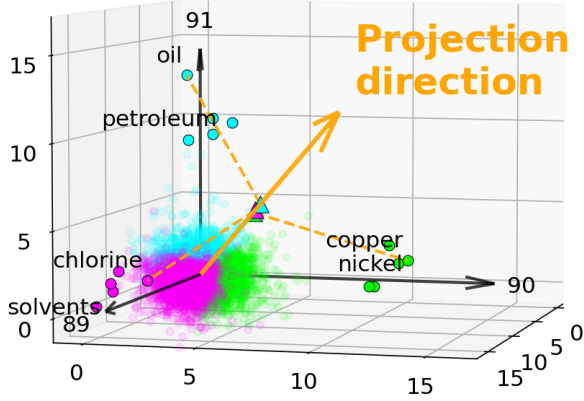


Figure 7: Projection of the subspace spanned by three consecutive axes in Fig. 1 into a one-dimensional space. Each word is assigned the color of the axis with the highest value. The projection direction is in the direction representing the subspace. For visualization, we randomly sampled 10,000 words, excluding the top five words on each axis.

## B.2 Projection from subspace to one-dimensional space

This section explains the projection from a subspace to a one-dimensional space using a specific example. Consider the subspace spanned by three consecutive axes (89, 90, 91) from Fig. 1. Figure 7 shows the projection of this subspace using  $f_r$ . The projection direction is in the direction representing the subspace, and the top words of each axis are projected close together.

## C Distribution of cosine similarity

Let us consider two random vectors  $X = (X_1, \dots, X_d), Y = (Y_1, \dots, Y_d) \in \mathbb{R}^d$  with elements of mean zero  $\mathbb{E}(X_\ell) = \mathbb{E}(Y_\ell) = 0$  and finite variance  $\mathbb{E}(X_\ell^2) = \sigma_X^2, \mathbb{E}(Y_\ell^2) = \sigma_Y^2$ . We assume that the elements  $X_1, \dots, X_d$  and  $Y_1, \dots, Y_d$  are independent, and the sequence  $X_1 Y_1, \dots, X_d Y_d$  satisfies Lindeberg's condition (Billingsley, 1995); for  $Z_\ell = X_\ell Y_\ell / \sigma_X \sigma_Y, \forall \epsilon > 0, \lim_{d \rightarrow \infty} d^{-1} \sum_{\ell=1}^d \mathbb{E} \left[ Z_\ell^2 1(|Z_\ell| > \epsilon \sqrt{d}) \right] = 0$ . Lindeberg's condition means no one  $X_\ell Y_\ell$  dominates the inner product  $\langle X, Y \rangle = \sum_{\ell=1}^d X_\ell Y_\ell$ , and it is satisfied, for example, when all the elements follow the identical distribution.

Then, for sufficiently large  $d$ , the cosine similarity  $\cos(X, Y)$  asymptotically follows  $\mathcal{N}(0, 1/d)$ , the normal distribution with mean 0 and variance  $1/d$ . In other words, for sufficiently large  $d$ ,

$$\sqrt{d} \cos(X, Y) \sim \mathcal{N}(0, 1). \quad (14)$$

This is easily shown as follows. First note that  $\mathbb{E}(X_\ell Y_\ell) = \mathbb{E}(X_\ell) \mathbb{E}(Y_\ell) = 0, \mathbb{E}(X_\ell^2 Y_\ell^2) = \mathbb{E}(X_\ell^2) \mathbb{E}(Y_\ell^2) = \sigma_X^2 \sigma_Y^2$ . Thus the inner product, if scaled by dimension,  $d^{-1/2} \langle X, Y \rangle = d^{-1/2} \sum_{\ell=1}^d X_\ell Y_\ell$  has mean zero and variance  $\sigma_X^2 \sigma_Y^2$ . Furthermore, according to the Lindeberg-Feller Central Limit Theorem, the distribution of the inner product asymptotically converges to the normal distribution as  $d$  grows large:

$$d^{-1/2} \langle X, Y \rangle \sim \mathcal{N}(0, \sigma_X^2 \sigma_Y^2). \quad (15)$$

It also follows from the law of large numbers,  $d^{-1} \|X\|^2 = d^{-1} \sum_{\ell=1}^d X_\ell^2$  converges in probability to  $\mathbb{E}(X_\ell^2) = \sigma_X^2$ . Similarly  $d^{-1} \|Y\|^2 \rightarrow \sigma_Y^2$  in probability. Therefore,

$$\sqrt{d} \cos(X, Y) = \frac{d^{-1/2} \langle X, Y \rangle}{\sqrt{d^{-1} \|X\|^2} \sqrt{d^{-1} \|Y\|^2}}$$

converges to  $d^{-1/2} \langle X, Y \rangle / \sigma_X \sigma_Y$  in probability, and thus (15) gives (14).

## D Details of dimensionality reduction experiments in Section 5

### D.1 Detailed explanation of each task

**Analogy task.** The embedding of the word  $i$  is denoted by  $y_i \in \mathbb{R}^d$ . We used the Google Analogy Test Set (Mikolov et al., 2013a), which contains 14 types of analogy tasks, and the Microsoft Research Syntactic Analogies Dataset (Mikolov et al., 2013c), which contains 16 types of analogy tasks. In the analogy tasks, the quality of the embeddings is evaluated by inferring word<sub>4</sub> to which word<sub>3</sub> corresponds if word<sub>1</sub> corresponds to word<sub>2</sub>. We compute the vector  $y_2 - y_1 + y_3$  and see if the closest embedding is  $y_4$  (top1 accuracy).

**Word similarity task.** We used MEN (Bruni et al., 2014), MTurk (Radinsky et al., 2011), RG65 (Rubenstein and Goodenough, 1965), RW (Luong et al., 2013), SimLex999 (Hill et al., 2015), WS353 (Finkelstein et al., 2002), WS353R (WS353 Relatedness), and WS353S (WS353 Similarity). In the word similarity tasks, the quality of the embeddings is evaluated by measuring the cosine similarity of the word embeddings and comparing it to the human-rated similarity scores. As the evaluation metric, we used Spearman's rank correlation coefficient between the human ratings and the cosine similarity.

Tasks	$p = 5$				$p = 20$				$p = 100$				$p = 300$
	PCA	Rand.	Skew.	Tour.	PCA	Rand.	Skew.	Tour.	PCA	Rand.	Skew.	Tour.	All
capital-common-countries	0.00	0.00	0.00	0.00	0.37	0.00	0.06	0.11	0.95	0.56	0.85	0.87	0.95
capital-world	0.00	0.00	0.00	0.00	0.26	0.02	0.05	0.11	0.90	0.73	0.80	0.82	0.95
city-in-state	0.00	0.00	0.00	0.00	0.03	0.00	0.02	0.04	0.42	0.28	0.24	0.40	0.67
currency	0.00	0.00	0.00	0.00	0.02	0.00	0.00	0.02	0.09	0.08	0.08	0.10	0.12
family	0.01	0.00	0.00	0.00	0.40	0.02	0.08	0.22	0.78	0.68	0.80	0.75	0.88
gram1-adjective-to-adverb	0.00	0.00	0.00	0.00	0.01	0.00	0.01	0.01	0.08	0.08	0.14	0.09	0.21
gram2-opposite	0.00	0.00	0.00	0.00	0.00	0.00	0.00	0.00	0.14	0.12	0.18	0.14	0.26
gram3-comparative	0.00	0.00	0.00	0.00	0.05	0.01	0.04	0.11	0.62	0.46	0.58	0.66	0.88
gram4-superlative	0.00	0.00	0.00	0.00	0.01	0.00	0.00	0.01	0.31	0.54	0.23	0.31	0.69
gram5-present-participle	0.00	0.00	0.00	0.00	0.03	0.00	0.03	0.07	0.44	0.30	0.59	0.58	0.69
gram6-nationality-adjective	0.00	0.00	0.00	0.00	0.57	0.07	0.22	0.43	0.91	0.88	0.91	0.88	0.93
gram7-past-tense	0.00	0.00	0.00	0.00	0.05	0.02	0.04	0.06	0.45	0.36	0.47	0.51	0.60
gram8-plural	0.00	0.00	0.00	0.00	0.11	0.01	0.04	0.07	0.73	0.40	0.59	0.56	0.76
gram9-plural-verbs	0.00	0.00	0.00	0.00	0.06	0.01	0.02	0.06	0.39	0.27	0.29	0.53	0.58
jj_jjr	0.00	0.00	0.00	0.00	0.01	0.00	0.01	0.03	0.35	0.23	0.29	0.43	0.66
jj_jjs	0.00	0.00	0.00	0.00	0.01	0.00	0.00	0.01	0.21	0.36	0.14	0.20	0.51
jjr_ij	0.00	0.00	0.00	0.00	0.01	0.00	0.03	0.02	0.33	0.27	0.32	0.33	0.54
jjr_jjs	0.00	0.00	0.00	0.00	0.01	0.00	0.01	0.01	0.24	0.37	0.15	0.20	0.55
jjs_ij	0.00	0.00	0.00	0.00	0.01	0.00	0.01	0.01	0.21	0.13	0.18	0.19	0.48
jjs_jjr	0.00	0.00	0.00	0.00	0.01	0.00	0.01	0.01	0.29	0.16	0.25	0.33	0.63
nn_nnpos	0.00	0.00	0.00	0.00	0.05	0.01	0.01	0.04	0.35	0.20	0.29	0.28	0.42
nn_nns	0.00	0.00	0.00	0.00	0.04	0.00	0.04	0.06	0.55	0.33	0.49	0.51	0.74
nnpos_nn	0.00	0.00	0.00	0.00	0.03	0.00	0.02	0.06	0.40	0.20	0.34	0.31	0.45
nns_nn	0.00	0.00	0.00	0.00	0.05	0.00	0.04	0.06	0.48	0.30	0.43	0.44	0.64
vb_vbd	0.00	0.00	0.00	0.00	0.11	0.03	0.09	0.07	0.45	0.36	0.40	0.54	0.58
vb_vbz	0.00	0.00	0.00	0.00	0.09	0.02	0.05	0.08	0.58	0.33	0.50	0.68	0.76
vbd_vb	0.00	0.00	0.00	0.00	0.09	0.04	0.12	0.08	0.46	0.36	0.56	0.56	0.69
vbd_vbz	0.00	0.00	0.00	0.00	0.08	0.01	0.04	0.05	0.48	0.26	0.38	0.54	0.63
vbz_vb	0.00	0.00	0.00	0.00	0.06	0.02	0.06	0.11	0.65	0.43	0.70	0.70	0.82
vbz_vbd	0.00	0.00	0.00	0.00	0.05	0.01	0.03	0.05	0.33	0.33	0.42	0.44	0.55
Average	0.00	0.00	0.00	0.00	<b>0.09</b>	0.01	0.04	0.07	0.45	0.34	0.42	<b>0.46</b>	0.63
MEN	0.16	0.19	0.11	0.35	0.32	0.33	0.29	0.51	0.66	0.56	0.63	0.66	0.75
MTurk	0.17	0.08	0.12	0.32	0.38	0.32	0.30	0.52	0.57	0.53	0.57	0.61	0.64
RG65	0.31	0.09	0.05	0.29	0.36	0.42	0.28	0.50	0.68	0.66	0.59	0.63	0.78
RW	0.09	0.10	0.07	0.13	0.14	0.16	0.10	0.25	0.24	0.32	0.28	0.30	0.34
SimLex999	0.01	0.13	0.04	0.07	0.11	0.21	0.08	0.21	0.27	0.37	0.28	0.31	0.40
WS353	0.12	0.16	0.02	0.31	0.15	0.28	0.18	0.44	0.47	0.40	0.43	0.52	0.57
WS353R	0.12	0.14	0.01	0.17	0.15	0.16	0.15	0.35	0.40	0.28	0.35	0.44	0.51
WS353S	0.18	0.21	0.06	0.45	0.21	0.35	0.26	0.55	0.57	0.51	0.58	0.62	0.69
Average	0.15	0.14	0.06	<b>0.26</b>	0.23	0.28	0.20	<b>0.42</b>	0.48	0.45	0.46	<b>0.51</b>	0.59
AP	0.33	0.22	0.22	0.27	0.36	0.26	0.28	0.40	0.51	0.45	0.54	0.56	0.66
BLESS	0.31	0.28	0.27	0.36	0.42	0.36	0.35	0.51	0.73	0.68	0.69	0.76	0.79
Battig	0.18	0.10	0.12	0.15	0.24	0.14	0.16	0.22	0.37	0.29	0.35	0.34	0.42
ESSLI_1a	0.50	0.41	0.45	0.64	0.61	0.57	0.48	0.77	0.73	0.59	0.73	0.75	0.70
ESSLI_2b	0.47	0.62	0.45	0.53	0.73	0.68	0.55	0.68	0.75	0.75	0.70	0.75	0.78
ESSLI_2c	0.44	0.44	0.42	0.44	0.53	0.60	0.49	0.56	0.58	0.53	0.60	0.60	0.58
Average	0.37	0.35	0.32	<b>0.40</b>	0.48	0.44	0.38	<b>0.52</b>	0.61	0.55	0.60	<b>0.63</b>	0.65

Table 3: The performance of dimensionality reduction for  $p$ -dimensional embeddings. *Rand.* stands for Random Order, *Skew.* for Skewness Sort, and *Tour.* for Axis Tour. The values in the table correspond to top 1 accuracy for analogy tasks, Spearman’s rank correlation for word similarity tasks, and purity for categorization tasks. Note that at  $p = 300$ , all embeddings give the same results.

**Categorization task.** We used AP (Almuhareb and Poesio, 2005), BLESS (Baroni and Lenci, 2011), Battig (Battig and Montague, 1969), ESSLLI\_1a (Baroni et al., 2008), ESSLLI\_2b (Baroni et al., 2008), and ESSLLI\_2c (Baroni et al., 2008). In the categorization tasks, the quality of the embeddings is evaluated by clustering them in the setting where each word is assigned a class label. As the evaluation metric, we used Purity, which shows the proportion of the most frequent class in the clusters. As clustering methods, we used

Hierarchical Clustering with five settings<sup>14</sup> and  $K$ -means<sup>15</sup>, and then selected the one that gave the highest purity.

## D.2 Results

Table 3 shows detailed experimental results of PCA, Random Order, Skewness Sort, and Axis Tour at

<sup>14</sup>By default, Word Embedding Benchmark uses the following affinity and linkage pairs for hierarchical clustering: (affinity, linkage) = (euclidean, ward), (euclidean, average), (euclidean, complete), (cosine, average), (cosine, complete).

<sup>15</sup>We used the same seed for all experiments.

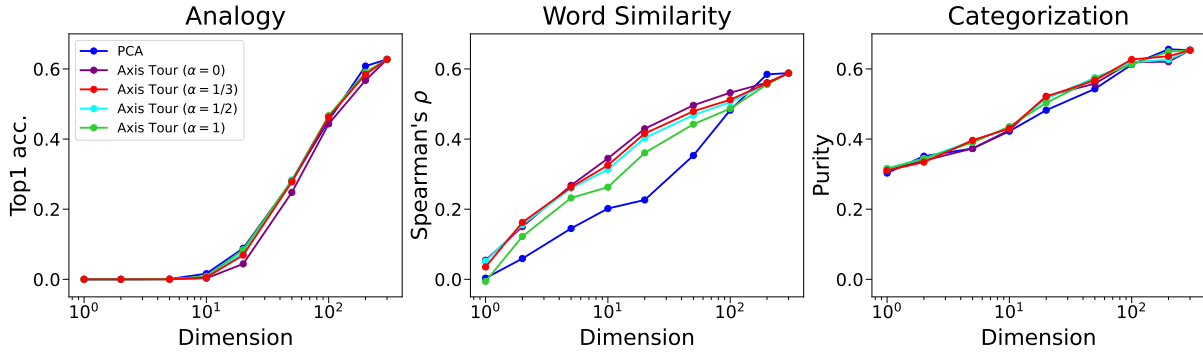


Figure 8: The performance of dimensionality reduction for the PCA-transformed embeddings and the Axis Tour embeddings with  $\alpha = 0, 1/3, 1/2, 1$ . Each value represents the average of 30 analogy tasks, 8 word similarity tasks, or 6 categorization tasks.

$p = 5, 20, 100, 300$  for each task. As already seen, Fig. 4 in Section 5 shows the average of each task at  $p = 1, 2, 5, 10, 20, 50, 100, 200, 300$  for the embeddings.

The Axis Tour embeddings showed superior performance in the word similarity tasks and the categorization tasks for almost all dimensions compared to other methods. In the analogy tasks, the Axis Tour embeddings achieved performance comparable to PCA and better than Random Order and Skewness Sort in most dimensions.

### D.3 Setting of $p = d (= 300)$

Note that the experimental results are the same for all embeddings for  $p = 300$ . First, as we saw in Appendix B.1, when  $p = d (= 300)$ , the matrix  $\mathbf{TF}$  (i.e., the projected  $p$ -dimensional embeddings) is equal to the matrix  $\mathbf{T}$  (i.e., the  $d$ -dimensional Axis Tour embeddings). Then, by definition, Axis Tour, Random Order, and Skewness Sort are the embeddings obtained by reordering the axes of the ICA-transformed embeddings and flipping their signs as needed. Thus, these three can be seen as the embeddings obtained by applying an orthogonal matrix to the ICA-transformed embeddings. Since the ICA-transformed embeddings are derived from the PCA-transformed embeddings by applying an orthogonal matrix<sup>16</sup>, cosine similarity and Euclidean distance remain unchanged for PCA, Random Order, Skewness Sort, and Axis Tour, leading to identical results in downstream tasks.

<sup>16</sup>Refer to the previous work for the relationship between PCA and ICA (Yamaguchi et al., 2023).

## E Additional experiments

### E.1 Qualitative observations for all axes of the Axis Tour embeddings

In Table 1, we used 300-dimensional GloVe and showed the semantic continuity of the axes of the Axis Tour embeddings, with illustrative examples of the meaning of *countries* (the 23rd axis to the 31st axis), *law* (the 101st axis to the 109th axis), and *art* (the 237th axis to the 245th axis). This section presents the top five words of the normalized embeddings across all 300 axes in Tables 4, 5, and 6.

For example, in Table 4, the 45th and 46th axes are related to *soccer*, the 47th axis to *golf*, the 48th axis to *tennis*, the 49th and 50th axes to *scores*, the 51st axis to *American football*, the 52nd axis to *basketball*, and the 53rd axis to *baseball*. These axes illustrate the semantic continuity across *sports*.

In Table 5, the 129th to the 140th axes are related to *numbers*. It is also interesting to note that the top words of each axis have similar numerical scales, highlighting how well the axis of the ICA-transformed embeddings captures meaning. In addition, the meaning of each axis changes continuously, much like a game of word association: the 219th axis relates to *colors*, the 220th axis to *light*, the 221st axis to *space*, the 222nd axis to *airplanes*, the 223rd axis to *ships*, the 224th axis to *storms*, the 225th axis to *weather*, the 226th axis to *biomes*, the 227th axis to *plants*.

In Table 6, the 272nd to the 289th axes are related to *personal names* from different linguistic regions as if this were a cluster of the meaning.

Note that due to space limitations, the top 1 and top 3 words on the 185th axis are truncated because they are repetitive symbols, and that URLs, email addresses, and phone numbers are anonymized.

0	1	2	3	4	5	6	7	8	9
phaen sandretto nakhchivan burghardt regno	region goriška languedoc regions saguenay-lac-saint-jean	mountain mount mountains everest peaks	stage vinokourov vuelta stages magicians	italy italian di francesco pietro	juan spain luis gonzález garcía	da são paulo joão janeiro	state terengganu kedah perlis kelantan	india indian singh shri delhi	vaas jayasuriya wicket jayawardene kallis
10	11	12	13	14	15	16	17	18	19
andrew divoff vanwyngarden hruska hampsten	chief executive ceo justiceship hienonen	general then-attorney gen. sindiso jiyane	bhavsar beppe ayme kahrd ripstein	spearritt 297.00 moçambique epoca huajun	contributed sebti avet aygin toosi	by sivuyile mulyanda boonradom tolkun	***.com tburr fluto ***.com ***.com	micro-history 1977-2010 1951-1972 qc8 1977-2006	family lythraceae wicket chrysobalanaceae polyporaceae pyronemataceae
20	21	22	23	24	25	26	27	28	29
order neoptera boletales svu poverelle	the macdougalls powhatans andhras sasanians	hungarians ethnic asians tatars berbers	serb bosnian croatia croatian serbian	russian russia moscow sergei aleksandr	czech prague poland polish warsaw	germany german berlin von cologne	france french le paris du	canada canadian ontario quebec saskatchewan	australia australian queensland brisbane perth
30	31	32	33	34	35	36	37	38	39
wiltshire shrewsbury lincolnshire peterborough croydon	liga relegated f.c. serie	coach coaching scolari vogts capello	frank capra sinatra wisner aigbogun	tony ianno canzoneri oursler kornheiser	mike johanns feters petke lupica	michael finnissy cerveris stuhlbarg tomasky	joseph joe macenka papp nollekens	jack palance o'lantern spring-heeled lemmon	&amp; llp amp & firm
40	41	42	43	44	45	46	47	48	49
analyst strategist securities hyoty udomsirikul	an rohp average-sized waidhofen taisce	three-week 20-minute two-week two-month 15-minute	festivities celebration celebrations commemoration ceremonies	27th 22nd 26th 23rd 35th	striker equalized midfielder header equalised	goalkeeper keeper goalie goaltender jaaskelainen	mickelson furyk els faldo woods	6-4 7-5 roddick kafelnikov dementieva	2-9 8-8 1-9 4-12 17-65
50	51	52	53	54	55	56	57	58	59
24-14 24-17 14-10 20-10 27-17	touchdown quarterback touchdowns qb interceptions	rebounds hardaway pippen shaquille medyess	inning hitter pitcher outfielder baseman	.301 .292 .293 .289 .288	9-for-13 3-for-8 5-for-12 4-for-11 12-of-19	on premiered picturized ixnay gorging	island islands fuerteventura conanicut wangerooge	greek greece athens greeks zeus	george takei stroubouloupoulos w.bush maharis
60	61	62	63	64	65	66	67	68	69
president teburoro vice bagbandy issayas	burundi uganda tanzania kenya zambia	envoys talks envoy annan solana	between relationship quarrel rivalry relationships	brouhaha over editorship dispute damocles	challenges dilemmas confronting dilemma vexing	numerous various sundry other mishaps	mistake error mistakes misjudgments disregard	horrific terrible horrendous horrible unspeakable	vitriolic racist denouncing strident insults
70	71	72	73	74	75	76	77	78	79
disgust anger feelings sadness revulsion	tenacity humility toughness newfound professionalism	informs destroys sustains confronts goes	life expectancies commuted transience great-west	their our forbears fellow-citizens its	arguably liveliest costliest quietest best-preserved	livelier nastier rougher prettier deadlier	conclusive corroboration no substantiation scant	endear semblance wobbled shaky unscathed	slowing slowdown weakening sluggish decline
80	81	82	83	84	85	86	87	88	89
index asx ase fise klse	1.48 1.62 2.07 2.05 1.67	20.45 15.55 33.65 13.45 17.35	30-year yield bond 10-year yields	2 1 teaspoons 3 teaspoon	sauce cooked cheese roasted bread	beer drink drinks brewed drinkers	antidepressant drugs drug medications prozac	proteins protein genes gene rna	chlorine solvents ammonia liquid flammable
90	91	92	93	94	95	96	97	98	99
copper nickel manganese molybdenum ore	oil petroleum oilfields crude pemex	power electricity substation hydroelectric megawatts	line railway lines arbatsko-pokrovskaya kolsás	road highway route north-south two-lane	three-story brick facade two-story building	hotel hotels resort resorts marriott	stores store grocery supermarkets retailer	industry export manufacturing distributors shoemaking	subsidiary company maker alcatel corp.
100	101	102	103	104	105	106	107	108	109
hedge fund funds investments investing	pay fees payments payment paid	land property lands estate bergisches	laws regulations enacted law provisions	court judge appellate appeals supreme	lawsuits lawsuit litigation suits suit	charges alleged prosecutors indicted convicted	camp prison buchenwald camps inmates	corpses corpse exhumed dismembered bodies	remain remained stayed stubbornly stays
110	111	112	113	114	115	116	117	118	119
hopelessly frustrated woefully hamstrung chronically	incredibly amazingly extremely very wonderfully	ingenious devious clever intricate cunning	to intend able humiliate try	fostering initiatives sustainable empowering entrepreneurship	tricking busily concentrating classifying disposing	into morphed transmuted degenerates delving	has had been consistently reinvented	19,583 21,563 16,875 20,833 30,313	3,048 dolne prateek bugis gumbinnen

Table 4: The top five words for the 0th axis to the 119th axis when we apply Axis Tour to 300-dimensional GloVe.

120	121	122	123	124	125	126	127	128	129
system systems renin-angiogensin centralized computerised	desktop macintosh pc software server	phone cellular cellphone telephone wireless	web sites site online myspace	television tv channel broadcast cbs	2300 12:30 11:30 0330 0930	4:23 2:47 2:33 8:38 2:21	_ ondeck holimont hawksnest belleyre	new york orleansians orleans-based n.y.	121.58 114.78 121.22 119.76 106.12
130	131	132	133	134	135	136	137	138	139
seventies sixties 2010s 1800s early	2001-2003 2003-2005 1999-2001 1998-2001 1995-1997	four five three eleven six	89 83 86 85 88	445 244 285 292 344	1,149 4,461 1,737 1,701 1,109	209.6 218.8 218.3 308.9 246.3	95.3 96.2 89.8 89.9 93.1	28.4 23.1 23.9 26.1 27.6	5.5 4.8 5.7 4.4 4.6
140	141	142	143	144	145	146	147	148	149
23,000 110,000 39,000 43,000 48,000	union workers machinists unions teamsters	alike academics industrialists sociologists pundits	theories theory posited notions notion	church anglican episcopal congregations congregation	sex sexual homosexual heterosexual unmarried	actress wife mother daughter née	german-born newspaperman entrepreneur politician russian-born	old 35-year 14-year 50-year 22-year	multibillion 20-million multi-million 100-million multimillion
150	151	152	153	154	155	156	157	158	159
) ( .0358 3,7996 unitals	rights human aproteh zimrights pillay	group groups lashkar-e-jhangvi forzani harkat	force gendarmierie contingent 500-strong contingents	insurgents militants gunmen guerrillas forces	guns rifles gun caliber weapon	wheels wheel rudder brakes hydraulic	sedan sedans v8 turbocharged camry	schumacher barrichello massa ferrari raikkonen	preakness belmont filly baffert thoroughbred
160	161	162	163	164	165	166	167	168	169
400m 100m 200m freestyle 200-meter	sports sport softball volleyball soccer	welterweight heavyweight middleweight ibf wba	la cerva cenerentola ferrière louvière	que pero sus en una	basidiomycota gorlice empleos autovía pudiera	.2667 estrategia creado hirta a.m.-6	lb3 5lb 8lb lb7 4lb	drawno krosniewice brochów lubaczów pobiedziska	behshahr abyek ramian khamir javanrud
170	171	172	173	174	175	176	177	178	179
bank central nivard banks pboc	river ljubljanica tigris tributary rivers	lake mývatn erhai chilka waramaug	city ozamis malaybalay phenix hitec	international airport tocumen gökçen aiport	thailand thai nakhon bangkok thais	minister prime minster minsiter interior	spokesman faizasyah cirtek tsanchev ladsous	nafez sedvill british-controlled videoton 2-6-2	adtac coronae mahalleh decarboxylase poderoso
180	181	182	183	184	185	186	187	188	189
8a-4p romik shefer samayoa hermanas	qeshlaqi dizaj-e kalayeh now-e patryan	automoviles vx-6 ***.***.*** principalmente yengejeh	jreyes ilovar hohtz ray-finned odalovic	***.***.*** .0210 ***.***.*** ***@***.com 65stk	_____... interbk ooooo... ***.***.*** harrynimes	moodin ***.***.*** wehz prahnk eesah	- skway thoh kursk tsih	- bkh wc2006-asia manutid pickup5thgraf	: www.***.com http://www.***.org http://www.***.com http://www.***.org
190	191	192	193	194	195	196	197	198	199
;. priu su .8226 sa/b	sarā as chahār khvosh akbarābād	rd2 clientes weinzapfel desempleo gevar	ipnotinmx mordella significado sandwicencense ***.***.***	gibbosa pratylenchus bifrenaria fimbriatus laticeps	1507.50 .000663 analista ramnarine hām	ixmiquilpan ***@***.com .71078 jagdeep naab	prolegs grij macul rambusch yr.ago	masuku quartic havner shealy vidro	artayev autoori tayyab pareto zermelo
200	201	202	203	204	205	206	207	208	209
swaffham ***.***.*** ollivier zend cronulla-sutherland	phthalic chamba nguyên kinghorn matanuska-susitna	72-77 gildernew deanne ethelbert kether	magnifica compra qc7 kowalska handanovic	funderburke hintikka chofetz dany's opticians	cunxiao cunshen cunxu siyuan lanqing	wang zhang xu li liu	japan japanese tokyo akira takashi	south korean korea dakotans carolinians	park prenton ji-sung naturpark brefni
210	211	212	213	214	215	216	217	218	219
national winema jurnalul ranthambhore chiúa	parliament duma speaker 150-seat 500-seat	party janata bjp socialists ndp	polling electoral balloting election tallying	republican sen. gop republicans mccain	. . . but though even	i 'cause gonna yeah gosh	silently stared screamed yelled sobbing	trousers pants dresses dress wearing	whitish yellowish brownish greyish reddish-brown
220	221	222	223	224	225	226	227	228	229
ultraviolet infrared telescopes light wavelengths	spacecraft astronauts astronaut orbit	aircraft jet planes boeing f-15	vessel ship ships vessels boats	hurricane storm storms typhoon cyclone	temperatures humid chilly weather unseasonably	grasslands habitats soils marshes sediments	shrubs trees vines planted seedlings	mammals birds rabbits animals reptiles	virus h5n1 swine flu outbreak
230	231	232	233	234	235	236	237	238	239
diagnosed lung inflammation complications fractures	medical care hospital hospitals physician	undergo thorough undergoing evaluation undergone	survey surveys statistics gallup statistical	agency notimex kathpress bss telam	newspaper daily zeitung izvestia kommersant	ign popmatters allmusic reviewer gamespot	award awards awarded prize emmy	film films movie starring directed	superhero marvel spin-off superheroes characters

Table 5: The top five words for the 120th axis to the 239th axis when we apply Axis Tour to 300-dimensional GloVe.

240	241	242	243	244	245	246	247	248	249
album	piano	paintings	manuscript	language	name	formula_1	set	mark	brian
albums	violin	painting	biographies	languages	names	formula_2	aflame	high-water	trenchard-smith
band	cello	art	pages	pashto	surname	formula_3	10-cd	dindal	doyle-murray
self-titled	percussion	sculpture	book	colloquial	phrase	formula_4	setting	wainberg	cadd
ep	orchestral	watercolor	handwritten	dialect	misspelling	formula_5	4-cd	hoppus	donlevy
250	251	252	253	254	255	256	257	258	259
ireland	martin	peter	paul	john	“	bazzani	david	scott	2-54
belfast	scelzo	guillam	virilio	rhys-davies	”	looking-glass	pittu	livengood	cretier
irish	wansleben	shockheaded	ricoeur	canemaker	xff	mouret	proval	lobdell	veltman
mowlam	clunes	maffay	langmack	motson	‘	munro	margolick	gud	f.r.
northern	damm	rauhofer	celan	mcgahern	schizopolis	mármol	gorcyca	speedman	nahant
260	261	262	263	264	265	266	267	268	269
palm	county	calif.	school	university	1976	1853	february	king	alwaleed
beach	unincorporated	california	high	professor	1973	1852	october	sigismund	prince
fla.	dekalb	inglewood	elementary	graduate	1966	1847	december	iv	saudi
ostrowski	fayette	pasadena	pine-richland	doctorate	1968	1856	june	emperor	kingdom
broward	pulaski	pomona	jr/sr	faculty	1971	1854	april	iii	tupouto’a
270	271	272	273	274	275	276	277	278	279
ali	israel	daniel	swedish	thomas	william	charles	james	wilkison	nack
al	israeli	briere	sweden	kretschmann	mastrosimone	dutoit	frain	mudavadi	narrowly
mohammed	israelis	macivor	norwegian	aquinas	beaudine	grodin	roday	henwood	gyoergy
sheikh	netanyahu	gildenlöw	norway	quasthoff	fichtner	sheeler	luceno	hogzilla	khand
mohammad	aviv	balavoine	fredrik	finigar	saroyan	wuorinen	remar	mottola	vanak
280	281	282	283	284	285	286	287	288	289
nhls	janyk	vranjes	robert	van	chris	marchena	steve	shaara	richard
ba’asyir	tookie	kilvert	deniro	lieshout	volstad	staniforth	railsback	jeff	stoltzman
organizaciones	germanica	bukan	halmi	dijk	braide	kaboul	turre	shain	ayoade
yordanov	walthers	paratore	garrigus	zandt	bordano	pelzer	forbert	friesen	basehart
millán	adquisiciones	ponge	redford	tuyl	tidland	43.18	kimock	sharlet	sandomir
290	291	292	293	294	295	296	297	298	299
simon	malatesta	bilyaletdinov	.000106	nazione	olya	gearon	sirajul	wonk	kerberos
bocanegra	.0217	pouget	fhs	ba872	dodecahedral	mikuláš	overexcited	kappa	mckelvey
napier-bell	lockard	cytidine	colecovision	blouin	cih	bracigliano	nabhani	fraternity	wajir
vouet	330-pound	zhulali	ronghua	comunicacion	alnus	venero	then-reigning	godsmack	veg
callow	puji	bc4	yunlong	wachau	9.29	mariangela	karmichael	bibliophiles	pdca

Table 6: The top five words for the 240th axis to the 299th axis when we apply Axis Tour to 300-dimensional GloVe.

## E.2 Comparison of $\alpha$

Figure 8 shows the average of each task at  $p = 1, 2, 5, 10, 20, 50, 100, 200, 300$  for the PCA-transformed embeddings and the Axis Tour embeddings with  $\alpha = 0, 1/3, 1/2, 1$ .

From Fig. 8, we can see that the performance of the Axis Tour embeddings changes for each task, depending on  $\alpha$ . For example, when comparing across all  $\alpha$ , while  $\alpha = 0$  shows good performance on word similarity tasks and poor performance on analogy tasks,  $\alpha = 1$  shows the opposite.

These results suggest that the quality of low-dimensional embeddings by the Axis Tour embeddings depends on the vector  $\mathbf{f}_r$  for projection. However, the overall changes for each  $\alpha$  are not as large, and in all tasks the performance is better than or comparable to that of the PCA-transformed embeddings, indicating the ability to construct better or comparable low-dimensional embeddings compared to PCA.

## E.3 Comparisons of $k$

While we have done experiments for the Axis Tour with  $k = 100$  using 300-dimensional GloVe in

Section 5, when computing the axis embedding in (3), what is the appropriate value for  $k$ ?

For example, if  $k = 1$  and the top 1 word happens to have a meaning different from that of the axis, it is not desirable to define the axis embedding using only that word. Conversely, as  $k$  increases, the number of words with meanings different from that of the axis in the top  $k$  words also increases, hindering the ability of the axis embedding to represent the meaning of the axis. For example, in an extreme case where  $k = n$ ,  $\text{Top}_k^\ell$  becomes equal to  $[n]$ , and *all* axis embeddings become the mean vector of  $\hat{\mathbf{s}}_i$  over the vocabulary set. In this case, it is impossible to find the order that maximizes the semantic continuity of the axes.

In this section, to address these questions, we compare the metric for the semantic continuity of the axes, as defined in (4), for  $k = 1, 10, 100, 1000$ , and then perform qualitative observation and dimension reduction experiments.

### E.3.1 Selection of $k$

In preparation, we perform the Axis Tour for  $k_1 = 1, 10, 100, 1000$ , resulting in the embedding



matrices  $\mathbf{T}_1, \mathbf{T}_{10}, \mathbf{T}_{100}, \mathbf{T}_{1000}$ . In this section, we *redefine* the axis embedding for them with top  $k_2 = 1, 10, 100, 1000$ , then evaluate the metric for the semantic continuity of the axes and thus compare the quality of  $\mathbf{T}_{k_1}$ .

**Redefinition of axis embedding.** Similar to  $\hat{\mathbf{S}}$ , we define the matrix  $\hat{\mathbf{T}}_{k_1} \in \mathbb{R}^{n \times d}$  as the normalization of the embeddings  $\mathbf{T}_{k_1}$  with row vectors  $\hat{\mathbf{t}}_{k_1,i} = \mathbf{t}_{k_1,i} / \|\mathbf{t}_{k_1,i}\|$ . Here, the  $i$ -th word embedding of  $\mathbf{T}_{k_1}$  and  $\hat{\mathbf{T}}_{k_1}$  are denoted by  $\mathbf{t}_{k_1,i}, \hat{\mathbf{t}}_{k_1,i} \in \mathbb{R}^d$ , respectively. We compare the elements of the  $\ell$ -th axis of  $\hat{\mathbf{T}}_{k_1}$  and denote the index set of words corresponding to the top  $k_2$  elements as  $\text{Top}_{k_2}^\ell$ .

We redefine the  $\ell$ -th axis embedding  $\mathbf{v}_\ell(k_1, k_2)$  for  $k_1$  and  $k_2$  as follows:

$$\mathbf{v}_\ell(k_1, k_2) := \frac{1}{k_2} \sum_{i \in \text{Top}_{k_2}^\ell} \hat{\mathbf{t}}_{k_1,i} \in \mathbb{R}^d. \quad (16)$$

If  $k_2 = k_1$ , then  $\mathbf{v}_\ell(k_1, k_2)$  coincides with the axis embedding used in the Axis Tour optimization. In contrast, if  $k_2 \neq k_1$  and the semantic continuity of the axes is still observed for  $\mathbf{v}_\ell(k_1, k_2)$ , then  $\mathbf{T}_{k_1}$  can be considered as high-quality embeddings that are robust to changes for  $k_2$ .

**Semantic continuity of axes for  $\mathbf{v}_\ell(k_1, k_2)$ .** Using  $\mathbf{v}_\ell(k_1, k_2)$ , we define the metric for the semantic continuity of the axes for each  $k_1$  and  $k_2$  as follows:

$$c(k_1, k_2) := \frac{1}{d} \cos(\mathbf{v}_1(k_1, k_2), \mathbf{v}_d(k_1, k_2)) + \frac{1}{d} \sum_{\ell=1}^{d-1} \cos(\mathbf{v}_\ell(k_1, k_2), \mathbf{v}_{\ell+1}(k_1, k_2)). \quad (17)$$

Note that, unlike (4), the axes are already ordered by the Axis Tour using  $k_1$ . Furthermore, in (17), the sum of  $\cos(\mathbf{v}_\ell(k_1, k_2), \mathbf{v}_{\ell+1}(k_1, k_2))$  is divided by the dimension  $d$ , which can be interpreted as the average of the cosine similarities between adjacent axis embeddings  $\mathbf{v}_\ell(k_1, k_2)$  and  $\mathbf{v}_{\ell+1}(k_1, k_2)$ .

**Comparison method for  $k$ .** We aim to compare the quality of  $\mathbf{T}_{k_1}$ . To facilitate this, we define the univariate functions of  $k$  for  $k_1 = 1, 10, 100, 1000$ :

$$C_1(k) := c(1, k), \quad (18)$$

$$C_{10}(k) := c(10, k), \quad (19)$$

$$C_{100}(k) := c(100, k), \quad (20)$$

$$C_{1000}(k) := c(1000, k). \quad (21)$$

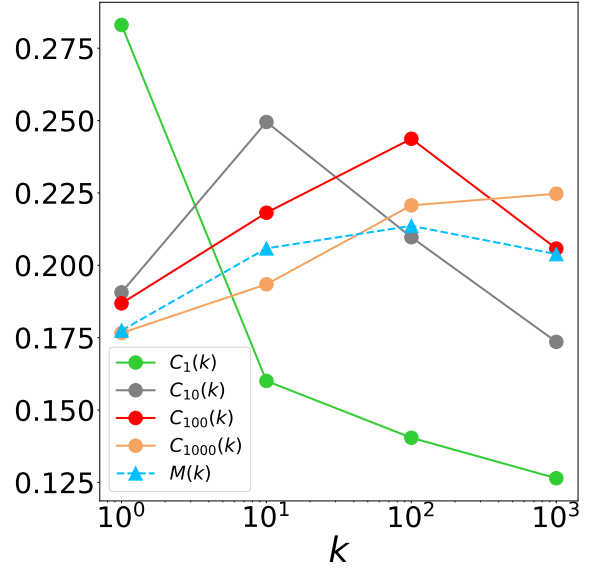


Figure 9: Plots of the functions  $C_1(k), C_{10}(k), C_{100}(k), C_{1000}(k)$  and  $M(k)$  for  $k = 1, 10, 100, 1000$ .

For example,  $C_1(k)$  in (18) is a function that measures the semantic continuity for the axis embedding  $\mathbf{v}_\ell(1, k)$  redefined by the top  $k$  words of the  $\ell$ -th axis of  $\mathbf{T}_1$ . To evaluate the robustness of  $\mathbf{T}_1$  to changes for  $k$ , we average the values of  $C_1(k)$  for  $k = 1, 10, 100, 1000$ . A higher average value indicates better quality.

The same explanation can be applied to  $\mathbf{T}_{10}, \mathbf{T}_{100}, \mathbf{T}_{1000}$ , which leads to the definition of a function  $M(k)$  for calculating these averages:

$$M(k) := \frac{C_k(1) + C_k(10) + C_k(100) + C_k(1000)}{4} \quad (22)$$

We compare  $M(1), M(10), M(100), M(1000)$  to evaluate the quality of  $\mathbf{T}_1, \mathbf{T}_{10}, \mathbf{T}_{100}, \mathbf{T}_{1000}$ .

**Results.** Figure 9 shows plots of the functions  $C_1(k), C_{10}(k), C_{100}(k), C_{1000}(k)$  and  $M(k)$  for  $k = 1, 10, 100, 1000$ .  $M(100)$  is the maximum value of  $M(k)$ . This result validates the use of  $k = 100$  as the default value for our experiment settings.

Furthermore,  $C_1(1)$  is the maximum value among  $C_1(k), C_{10}(k), C_{100}(k), C_{1000}(k)$  ( $k = 1, 10, 100, 1000$ ). In this setting, since we use the top 1 word of each axis for axis embedding, this Axis Tour is equivalent to the Word Tour of 300 words using cosine similarity distance. Thus, the axis embedding is identical to the word embedding, which avoids ambiguity and simplifies

237	238	239	240	241	242	243	244	245
india indian singh shri delhi	thailand thai nakhon bangkok thais	japan japanese tokyo akira takashi	germany german berlin von cologne	france french le paris du	italy italian di francesco pietro	ireland belfast irish mowlam northern	czech prague poland polish warsaw	hungarians ethnic asians tatars berbers
112	113	114	115	116	117	118	119	120
to intend able humiliate try	order neuroptera boletales svu poverelle	court judge appellate appeals supreme	charges alleged prosecutors indicted convicted	lawsuits lawsuit litigation suits suit	challenges dilemmas confronting dilemma vexing	remain remained stayed stubbornly stays	hopelessly frustrated woefully hamstrung chronically	incredibly amazingly extremely very wonderfully
220	221	222	223	224	225	226	227	228
sedan sedans v8 turbocharged camry	van lieshout dijk zandt tuyl	paintings painting art sculpture watercolor	manuscript biographies pages book handwritten	piano violin cello percussion orchestral	album albums band self-titled ep	award awards awarded prize emmy	actress wife mother daughter née	film films movie starring directed

(a)  $k = 1$ 

102	103	104	105	106	107	108	109	110
6-4 7-5 roddick kafelnikov dementieva	mickelson furyk els faldo woods	schumacher barrichello massa ferrari raikkonen	stage vinokourov vuelta stages magicians	france french le paris du	italy italian di francesco pietro	da são paulo joão janeiro	juan spain luis gonzález garcía	welterweight heavyweight middleweight ibf wba
199	200	201	202	203	204	205	206	207
between relationship quarrel rivalry relationships	sex sexual homosexual heterosexual unmarried	laws regulations enacted law provisions	court judge appellate appeals supreme	lawsuits lawsuit litigation suits suit	charges alleged prosecutors indicted convicted	camp prison buchenwald camps inmates	corpses corpse exhumed dismembered bodies	rights human aprodeh zimrights pillay
112	113	114	115	116	117	118	119	120
preakness belmont filly baffert thoroughbred	award awards awarded prize emmy	ign popmatters allmusic reviewer gamespot	album albums band self-titled ep	piano violin cello percussion orchestral	paintings painting art sculpture watercolor	manuscript biographies pages book handwritten	web sites site online myspace	phone cellular cellphone telephone wireless

(b)  $k = 10$ 

104	105	106	107	108	109	110	111	112
the maddockalls powhatans andhras sasanians	river jubljanica tigris tributary rivers	lake mývatn erhai chilka waramaug	canada canadian ontario quebec saskatchewan	france french le paris du	la cerva cenerentola ferrière louvière	italy italian di francesco pietro	stage vinokourov vuelta stages magicians	piano violin cello percussion orchestral
189	190	191	192	193	194	195	196	197
fostering initiatives sustainable empowering entrepreneurship	tricking busily concentrating classifying disposing	laws regulations enacted law provisions	court judge appellate appeals supreme	lawsuits lawsuit litigation suits suit	charges alleged prosecutors indicted convicted	camp prison buchenwald camps inmates	set afame 10-cd setting 4-cd	formula_1 formula_2 formula_3 formula_4 formula_5
108	109	110	111	112	113	114	115	116
france french le paris du	la cerva cenerentola ferrière louvière	italy italian di francesco pietro	stage vinokourov vuelta stages magicians	piano violin cello percussion orchestral	album albums band self-titled ep	superhero marvel spin-off superheroes characters	film films movie starring directed	“ ” xif ’ schizopolis

(c)  $k = 1000$ 

Table 7: Semantic continuity of axes by Axis Tour for normalized ICA-transformed embeddings. First, we focus on each central axis of Table 1 where  $k = 100$ . The axes are the 27th axis (*france, french, le, paris, du*), the 105th axis (*lawsuits, lawsuit, litigation, suits, suit*), and the 241st axis (*piano, violin, cello, percussion, orchestral*). This table then shows the top five words of the axes near these selected axes for  $k = 1, 10, 1000$ . Note that the axis indices change depending on the results of each Axis Tour.

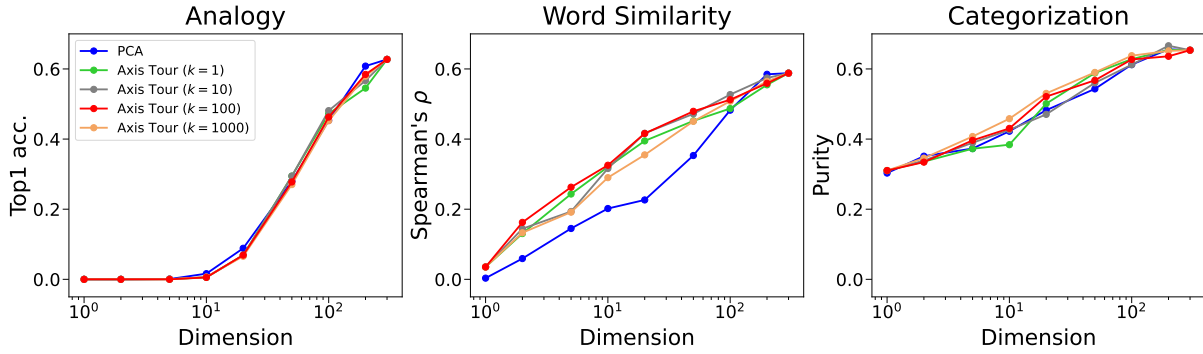


Figure 10: The performance of dimensionality reduction for the PCA-transformed embeddings and the Axis Tour embeddings with  $k = 1, 10, 100, 1000$  and  $\alpha = 1/3$ . Each value represents the average of 30 analogy tasks, 8 word similarity tasks, or 6 categorization tasks.

the task of finding semantically similar words. However, the lower value of  $M(1)$  compared to  $M(10)$ ,  $M(100)$ ,  $M(1000)$  illustrates the instability of representing the meaning of the axis by its top 1 word only.

### E.3.2 Qualitative observation

In Table 1, we observed examples of consecutive axes extracted from the Axis Tour embeddings with  $k = 100$ . These include the 27th axis (the top five words are *france*, *french*, *le*, *paris*, and *du*, so the *France* axis), the 105th axis (the top five words are *lawsuits*, *lawsuit*, *litigation*, *suits*, and *suit*, so the *lawsuit* axis), and the 241st axis (the top five words are *piano*, *violin*, *cello*, *percussion*, and *orchestral*, so the *music instruments* axis). Table 7 shows the axes close to these axes for  $k = 1, 10, 1000$ . Note that the axis indices change depending on the results of each Axis Tour.

For each  $k$ , even the same axis shows significant differences in the nearby axes. For example, at  $k = 1$ , in the bottom row, the meaning of the 227th axis is *female*, but since the top 1 word is *actress*, the axis is adjacent to the axes whose meanings are *award* and *movie*. This shows the disadvantage of the Axis Tour with  $k = 1$ . At  $k = 10$ , the top row shows that there are more axes related to *personal names* than to *countries* near the *France* axis compared to  $k = 100$ . At  $k = 1000$ , it is interesting to see that the axes *France* and *musical instruments*, which are far apart at  $k = 100$ , are close together.

Note that there is a selection bias in this comparison, as we use understandable examples for  $k = 100$  in Table 1 to compare with  $k = 1, 10, 1000$ .

### E.3.3 Dimensionality reduction

Figure 10 shows the average of each task at  $p = 1, 2, 5, 10, 20, 50, 100, 200, 300$  for the PCA-transformed embeddings and the Axis Tour embeddings with  $k = 1, 10, 100, 1000$  and  $\alpha = 1/3$ .

From Fig. 10 we can see that the performance of the Axis Tour embeddings changes for each task, depending on  $k$ . For example, when comparing across all  $k$ ,  $k = 1000$  shows good performance on categorization tasks and poor performance on word similarity tasks. In contrast, in lower dimensions,  $k = 1$  performs better on word similarity tasks than  $k = 1000$ , but shows worse performance on categorization tasks. While  $k = 100$  does not always show the top performance in all three tasks, it consistently shows stable performance.

These results suggest that the quality of low-dimensional embeddings by the Axis Tour embeddings depends on  $k$  for axis embedding.

### E.4 Dimensionality reduction by projection for Skewness Sort and Rand Order

The dimensionality reduction by projection in Section 4.3 can be applied not only to Axis Tour, but also to Skewness Sort and Random Order. Therefore, this section compares the dimensionality reduction method with those used for Skewness Sort and Random Order in Section 5.3, where the axes are selected sequentially from the first to last.

For the sake of explanation, let the embedding matrices for Skewness Sort and Random Order be denoted as  $\mathbf{S}_{\text{skew}}$  and  $\mathbf{S}_{\text{rand}}$ , respectively. Let the skewness of the  $\ell$ -th axis for each be  $\gamma_{\text{skew},\ell}, \gamma_{\text{rand},\ell} \in \mathbb{R}$ . By the definition of Skewness Sort,  $\gamma_{\text{skew},\ell} \geq 0$ . Similar to Section 4.3, we consider reducing the dimensions from  $d$  to  $p$  ( $p \leq d$ ), divide  $[d]$  into  $p$  equal-length intervals,

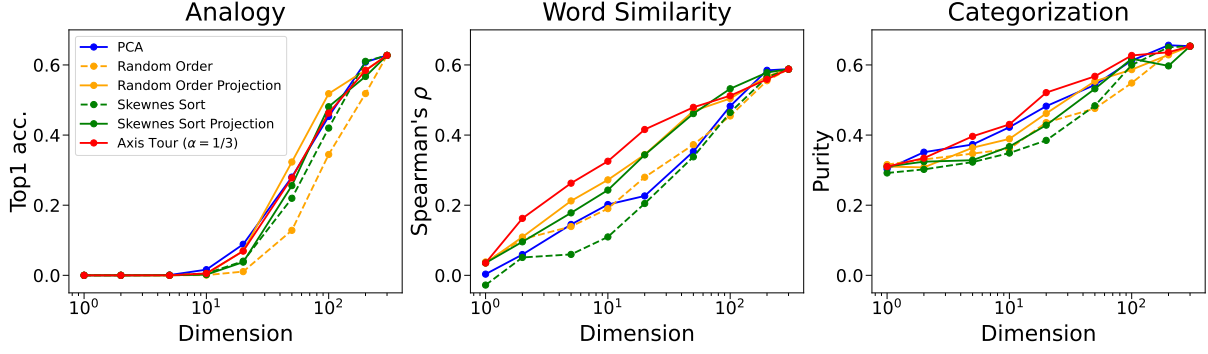


Figure 11: The performance of dimensionality reduction for the embeddings including Skewness Sort Projection and Random Order Projection with  $\alpha = 1/3$ . Each value represents the average of 30 analogy tasks, 8 word similarity tasks, or 6 categorization tasks.

and use the index set for the  $r$ -th interval  $I_r = \{a_r, \dots, b_r\}$  ( $a_r, b_r \in [d], a_r \leq b_r$ ).

#### E.4.1 Skewness Sort Projection

Given  $\gamma_{\text{skew},\ell} \geq 0$ , similar to  $\mathbf{f}_r = (f_r^{(\ell)})_{\ell=1}^d \in \mathbb{R}_{\geq 0}^d$  in (5), we define a unit vector  $\mathbf{f}_{\text{skew},r} = (f_{\text{skew},r}^{(\ell)})_{\ell=1}^d \in \mathbb{R}_{\geq 0}^d$  for each  $I_r$  as follows:

$$f_{\text{skew},r}^{(\ell)} = \begin{cases} \frac{\gamma_{\text{skew},\ell}^\alpha}{\sqrt{\sum_{m=a_r}^{b_r} \gamma_{\text{skew},m}^{2\alpha}}} & \text{for } \ell \in I_r \\ 0 & \text{otherwise,} \end{cases} \quad (23)$$

where  $\alpha \in \mathbb{R}_{\geq 0}$ . We then define  $\mathbf{F}_{\text{skew}} := [\mathbf{f}_{\text{skew},1}, \dots, \mathbf{f}_{\text{skew},p}] \in \mathbb{R}^{d \times p}$  and obtain the  $p$ -dimensional embedding matrix  $\mathbf{S}_{\text{skew}} \mathbf{F}_{\text{skew}} \in \mathbb{R}^{n \times p}$ . We call these embeddings as **Skewness Sort Projection**.

#### E.4.2 Random Order Projection

For the Random Order embeddings, some axes may have  $\gamma_{\text{rand},\ell} < 0$ . In this case,  $\gamma_{\text{skew},\ell}^\alpha$  may not be defined in  $\mathbb{R}$  for some  $\alpha \in \mathbb{R}_{\geq 0}$ . Consequently, we cannot directly use the definition of  $\mathbf{f}_r$  as a vector for projection. Therefore, even for the Random Order embedding matrix, we flip the sign of each axis to ensure that the skewness is positive, thereby defining a matrix for projection<sup>17</sup>. To do this, we define a unit vector  $\mathbf{f}_{\text{rand},r} = (f_{\text{rand},r}^{(\ell)})_{\ell=1}^d \in \mathbb{R}^d$  for each interval  $I_r$  as follows:

$$f_{\text{rand},r}^{(\ell)} = \begin{cases} \frac{\text{sgn}(\gamma_{\text{rand},\ell}) |\gamma_{\text{rand},\ell}|^\alpha}{\sqrt{\sum_{m=a_r}^{b_r} \gamma_{\text{rand},m}^{2\alpha}}} & \text{for } \ell \in I_r \\ 0 & \text{otherwise,} \end{cases} \quad (24)$$

<sup>17</sup>If the skewness of all axes in the Random Order matrix were initially set to be positive, this complex procedure could be avoided. However, our setup assumes that the sign and order of the axes are arbitrary after the ICA transformation, so the skewness of each axis of the matrix is not positive by default.

where  $\alpha \in \mathbb{R}_{\geq 0}$  and  $\text{sgn}(\cdot)$  represents the sign function. We then define  $\mathbf{F}_{\text{rand}} := [\mathbf{f}_{\text{rand},1}, \dots, \mathbf{f}_{\text{rand},p}] \in \mathbb{R}^{d \times p}$  and obtain the  $p$ -dimensional embedding matrix  $\mathbf{S}_{\text{rand}} \mathbf{F}_{\text{rand}} \in \mathbb{R}^{n \times p}$ . We call these embeddings as **Random Order Projection**.

#### E.4.3 Results

Similar to Axis Tour, we set the default value of  $\alpha$  to  $\alpha = 1/3$  for both Skewness Sort Projection and Random Order Projection. Figure 11 shows the average of each task at  $p = 1, 2, 5, 10, 20, 50, 100, 200, 300$  for the embeddings.

Dimensionality reduction for Axis Tour is still better than or nearly equivalent to Skewness Sort Projection and Random Order Projection for most dimensions in each task. Similar to the results in Section 5.3, these results also suggest the efficiency of dimensionality reduction for Axis Tour.

Note that both Skewness Sort Projection and Random Order Projection show performance improvements over Skewness Sort and Random Order in most dimensions. In particular, both show even better performance than PCA on word similarity tasks. This suggests that they are stronger baseline methods.

Interestingly, despite the lower performance of Random Order in analogy tasks, Random Order Projection performs slightly better than Axis Tour and PCA at  $p = 50, 100$ . Considering that Axis Tour showed only equivalent performance to PCA for even different  $\alpha$  in Fig. 8 or  $k$  in Fig. 10, this result suggests that by applying clustering or similar techniques to axis embeddings, we may obtain more effective low-dimensional vectors.

#### E.4.4 Setting of $p = d (= 300)$

When  $p = d$ , similar to Skewness Sort and Random Order, the performance of Skewness Sort Projection and Random Order Projection for each task is equivalent to that of PCA.

For Skewness Sort Projection, from (23) and the discussion in Appendix B.1, it can be shown that when  $p = d$ , we have  $\mathbf{F}_{\text{skew}} = \mathbf{I}$ , and therefore  $\mathbf{S}_{\text{skew}}\mathbf{F}_{\text{skew}} = \mathbf{S}_{\text{skew}}\mathbf{I} = \mathbf{S}_{\text{skew}}$ .

In preparation for Random Order Projection, we denote  $\mathbf{S}_{\text{rand}, \geq 0}$  as the matrix obtained by flipping the sign of each axis in  $\mathbf{S}_{\text{rand}}$  so that the skewness is positive. It then follows from the discussion in Appendix E.4.2 that, similar to the Skewness Sort Projection,  $\mathbf{S}_{\text{rand}}\mathbf{F}_{\text{rand}} = \mathbf{S}_{\text{rand}, \geq 0}\mathbf{I} = \mathbf{S}_{\text{rand}, \geq 0}$  when  $p = d$ . Thus, we can see that the performance of  $\mathbf{S}_{\text{rand}, \geq 0}$  is equivalent to that of  $\mathbf{S}_{\text{rand}}$  since  $\mathbf{S}_{\text{rand}, \geq 0}$  is derived from  $\mathbf{S}_{\text{rand}}$  by applying the orthogonal matrix to flip the sign of each axis.

#### E.5 Other embeddings

In Section 5, we used 300-dimensional GloVe<sup>18</sup> with  $n = 400,000$ . In this section, we extend our experiments to other embeddings. We used 300-dimensional word2vec<sup>19</sup> (Mikolov et al., 2013b) as static embeddings and 768-dimensional BERT<sup>20</sup> (Devlin et al., 2019) from the Hugging Face transformers library (Wolf et al., 2020) as dynamic embeddings.

For word2vec, given the original vocabulary size of three million, we selected only the top 40,000 words based on frequency after converting all words to lowercase. The word frequency information was obtained using wordfreq (Speer, 2022).

For BERT, we first input sentences from the One Billion Word Benchmark (Chelba et al., 2014) into BERT, and then used the first 40,000 tokens, including special tokens like [CLS] and [SEP]. It is important to note that the embeddings are different even for identical tokens, so we differentiated tokens like *cat* as *cat\_0*, *cat\_1*, and so on.

Similar to GloVe, for both word2vec and BERT, we set  $k = 100$  as the hyperparameter of the axis embedding for Axis Tour.

<sup>18</sup>The embeddings can be downloaded here: <https://nlp.stanford.edu/data/glove.6B.zip>.

<sup>19</sup><https://code.google.com/archive/p/word2vec/>

<sup>20</sup><https://huggingface.co/bert-base-uncased>

#### E.5.1 Qualitative observation

Tables 8a and 8b show the examples of the axes of the Axis Tour embeddings for word2vec and BERT, respectively. We can also see the semantic continuity of the axes of the Axis Tour embeddings for word2vec in Table 8a, just as we observed the semantic continuity of those for GloVe in Tables 4, 5 and 6. For BERT, the semantic continuity of the axes is also observed in Table 8b, although there are axes whose top tokens are the identical tokens. This is due to dynamic embeddings and differs from static embeddings as in GloVe and word2vec.

#### E.5.2 Scatterplots of Table 8

Figures 12 and 13 show the scatterplots of the two-dimensional projections for the axes of the Axis Tour embeddings for word2vec and BERT in Tables 8a and 8b, respectively. We used the procedure described in Appendix A.1. Similar to Figs. 1 and 6, for both word2vec and BERT, we can see that the top words of the axes are farther from the origin than those of the Skewness Sort, and the meanings of the adjacent axes change continuously.

For Figs. 12 and 13, Table 9 shows the values of  $d_I$  and  $c_I$  as the evaluation metrics defined in Appendix A.3. Similar to Table 2, for both word2vec and BERT, Axis Tour shows higher values for both  $d_I$  and  $c_I$  than Skewness Sort, indicating better projection quality.

#### E.5.3 Cosine similarity between adjacent axis embeddings

Figure 14 shows the histograms of  $\cos(\mathbf{v}_\ell, \mathbf{v}_{\ell+1})$  of the Axis Tour embeddings and the baseline embeddings for both word2vec and BERT. Similar to the results for GloVe in Fig. 2, the values of  $\cos(\mathbf{v}_\ell, \mathbf{v}_{\ell+1})$  are consistently higher in Axis Tour, while this trend is not observed in the other baselines.

Figures 15 and 16 illustrate the relationship between the skewness and the average of consecutive two cosine similarities for Axis Tour and Skewness Sort. Interestingly, while the Axis Tour embeddings for BERT show a strong correlation between the skewness and the average of two cosine similarities in Fig. 16a, similar to the results for GloVe in Fig. 5a, the Axis Tour embeddings for word2vec do not show such a correlation in Fig. 15a.

As future work, it may be interesting to consider the detailed relationship between the skewness and the cosine similarity between adjacent axis embeddings, as well as the relationship between the

50	51	52	53	54	55	56	57	58	59
frustration	mindset	aspects	problems	deteriorating	rise	went	was	sees	given
anger	philosophy	factors	difficulties	evolving	rising	slipped	has	gets	receive
resentment	attitudes	variables	hardships	urgent	spike	stumbled	requires	embraces	received
indignation	attitude	facets	shortcomings	rapidly	soar	ran	had	creates	give
unhappiness	worldview	elements	troubles	dire	rises	drifted	is	inspires	receiving
100	101	102	103	104	105	106	107	108	109
gameplay	gambling	filly	livestock	planting	birds	dog	babies	father	people
multiplayer	casino	colt	cattle	seedlings	species	dogs	infants	mother	americans
capcom	casinos	###-mile	farm	blooms	fish	puppy	newborn	siblings	britons
gamers	blackjack	mare	dairy	vines	bird	pet	newborns	son	patrons
zelda	gamblers	gr.3	cows	shrub	turtles	cats	baby	grandparents	viewers
150	151	152	153	154	155	156	157	158	159
dh`ing	pitched	assists	nba	pointer	header	everton	cambridgeshire	milford	allegheeny
batting_###	##/#-inning	steals	rondo	timeout	footed	arsenal	hertfordshire	westerly	harrisburg
ss/2b	innings	points	pistons	foul	deflected	tottenham	oxfordshire	marlborough	pennsylvania
of/1b	##/#innings	###_###_###	nets	jumper	angled	fulham	staffordshire	bridgewater	pa.
2b/of	outing	rebounds	nuggets	halftime	keeper	anfield	buckinghamshire	amherst	penn
200	201	202	203	204	205	206	207	208	209
proteins	psn###	pills	beer	restaurant	sauce	diet	instructor	school	sociology
protein	map####	drugs	whiskey	grill	soup	diets	teach	teachers	anthropology
enzyme	ap#####	heroin	lager	bistro	pasta	dieting	instruction	teacher	undergraduate
molecule	gw#####	morphine	beers	diners	saucos	nutrition	beginners	elementary	postgraduate
intracellular	ly#####	ecstasy	brewery	restaurants	meatballs	carbohydrate	training	pupils	phd
250	251	252	253	254	255	256	257	258	259
workers	gdp	budget	payments	tax	senate	primaries	bush	mps	ontario
###/hour	economists	cuts	payment	taxes	bill	democratic	obama	labour	bc
##.###/hr	inflation	deficit	pay	surcharge	d-tex.	voters	clinton	commons	saskatchewan
9/hour	cpi	budgets	paycheck	gst	rep.	election	cheney	tory	alberta
wages	ism	austerity	deductible	levies	r-md.	republican	putin	tories	canada

(a) word2vec

50	51	52	53	54	55	56	57	58	59
the_1336	air_7	rail_0	of_704	emerge_2	face_2	make_21	see_9	truth_0	takes_1
the_1335	aviation_0	service_0	the_900	to_350	emerge_0	look_2	know_3	truth_5	a_202
`_306	air_5	express_0	the_1609	a_281	find_1	double_5	knew_0	truth_2	maps_0
s_242	plane_1	the_191	the_901	the_723	yourself_0	sure_2	aware_5	share_10	sweep_0
it_137	jet_0	trans_0	the_1159	turn_3	to_189	make_26	know_5	truth_1	chronic_0
100	101	102	103	104	105	106	107	108	109
liverpool_1	lineup_1	some_8	little_2	five_0	four_6	2_9	both_1	between_12	agreement_0
annum_1	group_16	some_43	bit_2	two_14	six_0	two_47	both_10	between_9	an_82
shower_0	band_1	some_21	few_8	two_25	four_15	2_1	both_9	relations_1	struck_1
_755	group_2	many_5	bit_1	few_12	five_1	second_11	two_36	between_10	reached_1
liverpool_2	number_10	some_27	bit_0	three_9	five_6	two_0	both_6	bonding_0	talks_2
150	151	152	153	154	155	156	157	158	159
_115	_432	_1022	_1512	_114	a_159	r_0	asher_0	michael_1	emma_0
_701	_901	_181	_895	_1525	r_1	d_12	hilton_0	james_0	cindy_0
_172	_876	_180	_1260	_110	h_1	p_8	colt_0	peter_1	mare_0
_1526	_1561	_408	_1339	_1575	_381	m_12	##nie_4	mike_3	kate_0
_1527	_1367	_1024	_1055	_492	_600	v_0	jesse_0	mike_1	beth_0
200	201	202	203	204	205	206	207	208	209
software_1	services_3	limited_1	least_0	cannot_2	also_53	schools_5	bachelor_0	workers_4	users_2
software_2	capabilities_0	the_271	must_2	a_276	_613	students_4	degree_0	jobs_2	investors_7
hardware_0	services_2	are_26	a_98	any_10	cents_2	schools_1	the_739	workers_1	investors_1
software_0	services_4	to_141	[SEP]_190	in_256	government_29	student_2	major_8	workers_2	users_0
free_3	services_7	a_116	of_116	to_300	20_14	school_2	subjects_0	workers_10	users_3
250	251	252	253	254	255	256	257	258	259
time_9	year_57	hour_3	year_51	day_14	thursday_14	month_10	european_1	world_27	##_3
based_5	year_68	weeks_3	year_37	day_8	tuesday_6	week_10	european_6	world_31	their_17
lined_4	year_56	minutes_1	year_15	day_7	monday_8	year_67	european_0	world_7	nations_0
lined_2	year_59	hours_4	year_72	day_20	wednesday_3	week_0	european_3	world_17	countries_0
level_0	year_69	hour_5	year_13	day_2	thursday_0	saturday_0	european_5	world_5	[SEP]_249

(b) BERT

Table 8: Semantic continuity of axes by Axis Tour for normalized ICA-transformed embeddings. We apply Axis Tour to 300-dimensional word2vec and 768-dimensional BERT. For the 50th, 100th, 150th, 200th, and 250th axes, we extract ten consecutive axes from each of these axes and display the top five words for each of the extracted axes.

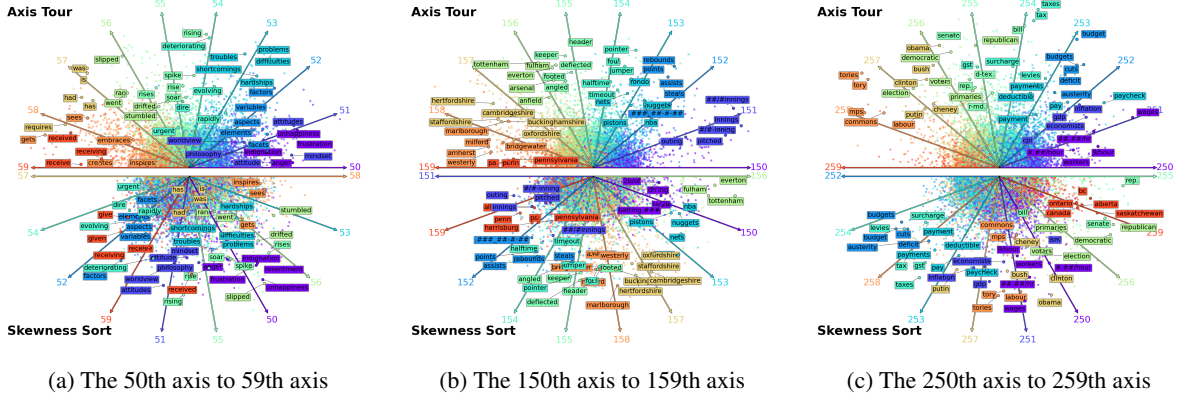


Figure 12: For word2vec, the scatterplots of the two-dimensional projections for the axes from the 50th to the 59th, from the 150th to the 159th, and from the 250th to the 259th in Table 8a.

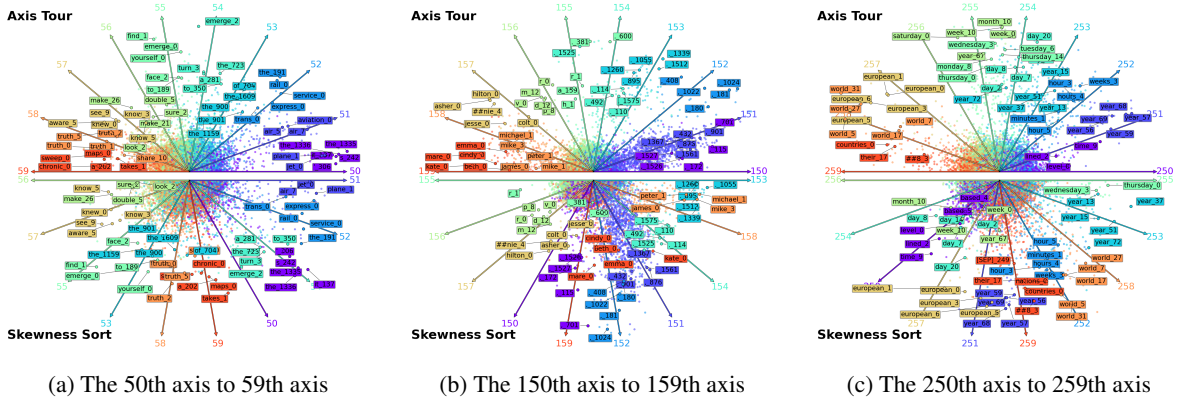


Figure 13: For BERT, the scatterplots of the two-dimensional projections for the axes from the 50th to the 59th, from the 150th to the 159th, and from the 250th to the 259th in Table 8b.

Fig.	Axis Tour		Skewness Sort	
	$d_I$	$c_I$	$d_I$	$c_I$
12a	0.70	0.30	0.55	0.00
12b	0.79	0.34	0.68	0.13
12c	0.80	0.27	0.71	0.05
13a	0.60	0.28	0.59	0.11
13b	0.71	0.33	0.60	0.06
13c	0.64	0.31	0.53	0.07

Table 9: The values of  $d_I$  and  $c_I$  for Figs. 12 and 13.

skewness and the strength of meaning of an axis.

#### E.5.4 Dimensionality reduction: analogy, word similarity, and categorization tasks

In this section, similar to Section 5.3, we evaluate the performance of dimensionality reduction using the method described in Section 4.3. It is important to note that since BERT embeddings are dynamic embeddings, the token embeddings obtained from

sentences in the One Billion Word Benchmark are different from those in each task. Therefore, this evaluation focuses only on word2vec embeddings.

Figure 17 shows the average of each task at  $p = 1, 2, 5, 10, 20, 50, 100, 200, 300$  for the embeddings derived from word2vec. Axis Tour outperformed both Random Order and Skewness Sort in each task. In analogy tasks, Axis Tour outperformed PCA in lower dimensions and was nearly equivalent in other dimensions.

Although PCA remains a strong baseline for analogy and categorization tasks because it is an efficient dimensionality reduction method, these results suggest that there is room for performance improvement. However, this study focused primarily on maximizing the semantic continuity of the axes in ICA-transformed embeddings. As mentioned in Limitations, it remains an area for future work to construct more efficient low-dimensional embeddings based on the axes in ICA-transformed embeddings.

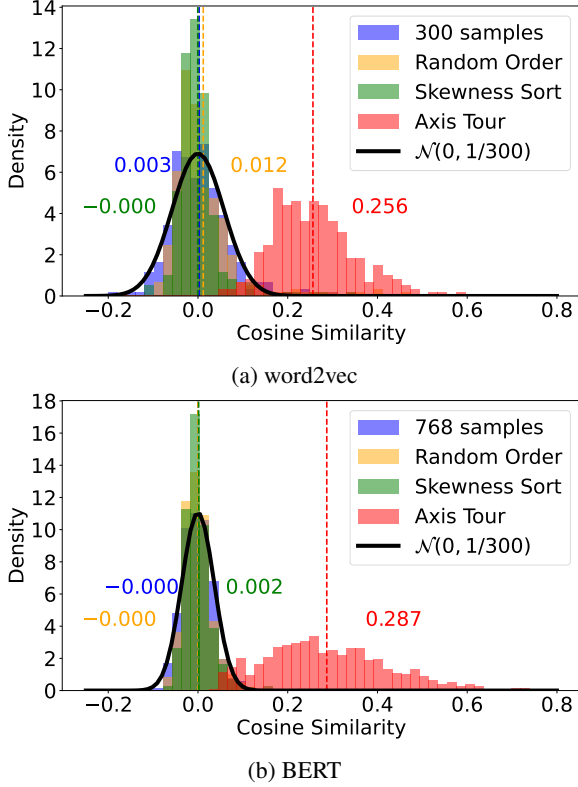


Figure 14: Histograms of  $\cos(\mathbf{v}_\ell, \mathbf{v}_{\ell+1})$  for word2vec and BERT. For BERT, we sampled 768 random words and drew the normal distribution  $\mathcal{N}(0, 1/768)$  instead of 300 words and the normal distribution  $\mathcal{N}(0, 1/300)$ . The rest of the procedure is the same as in Fig. 2.

## F Topographic ICA (TICA)

Our proposed method, Axis Tour, is related to Topographic Independent Component Analysis (TICA) (Kohonen, 2001; Hyvärinen et al., 2001a) in terms of ordering the axes of ICA-transformed embeddings, taking into account the sequential relationship between independent components. Therefore, this section first gives a brief overview of TICA. Then, we perform experiments on the TICA embeddings similar to those performed on the Axis Tour embeddings, and then show comparisons of Axis Tour and TICA.

### F.1 Overview of TICA

Topographic ICA (TICA) (Kohonen, 2001; Hyvärinen et al., 2001a) is a variant of linear ICA. While classic ICA assumes independence of the source components<sup>21</sup>  $\mathbf{s} = (s_\ell)_{\ell=1}^d \in \mathbb{R}^d$ , TICA allows for positive higher-order correlations  $\text{cov}(s_\ell^2, s_m^2)$

<sup>21</sup>Regarding the indices of the axes, the notation for  $\mathbf{f}_r = (f_r^{(\ell)})_{\ell=1}^d$ , as seen in the Section 4.3, would be written as  $\mathbf{s} = (s^{(\ell)})_{\ell=1}^d$ . However, for the sake of readability, this section uses the notation  $\mathbf{s} = (s_\ell)_{\ell=1}^d$ .

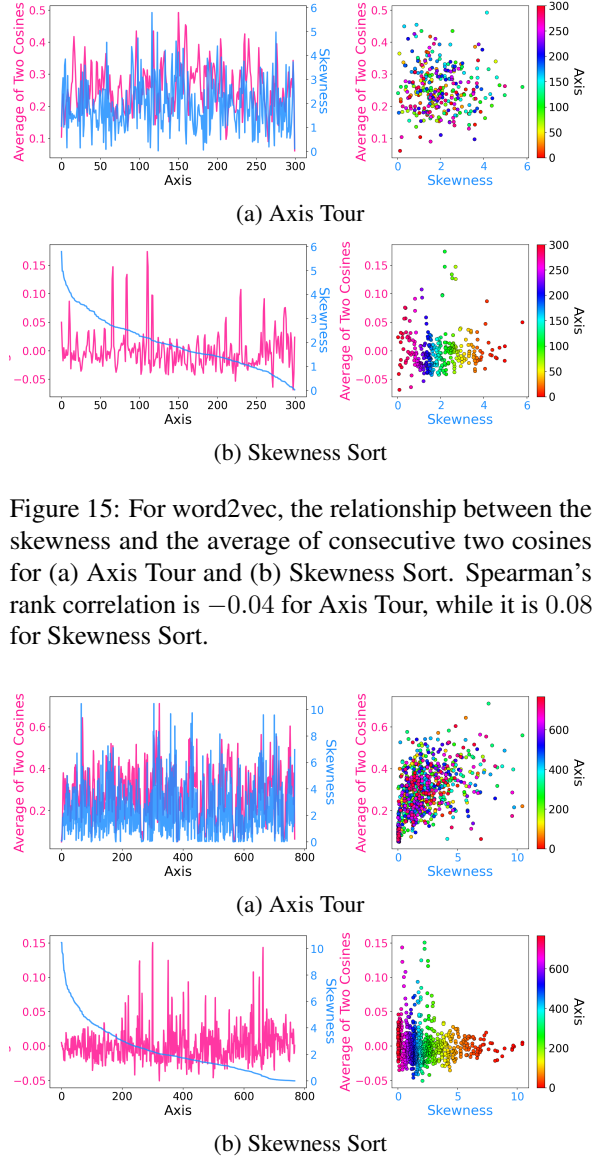


Figure 15: For word2vec, the relationship between the skewness and the average of consecutive two cosines for (a) Axis Tour and (b) Skewness Sort. Spearman’s rank correlation is  $-0.04$  for Axis Tour, while it is  $0.08$  for Skewness Sort.

Figure 16: For BERT, the relationship between the skewness and the average of consecutive two cosines for (a) Axis Tour and (b) Skewness Sort. Spearman’s rank correlation is  $0.50$  for Axis Tour, while it is  $-0.10$  for Skewness Sort.

and assumes that the variances of adjacent sources are correlated. In the probabilistic model of TICA, each variance  $\sigma_\ell^2$  of source component  $s_\ell$  is generated from the factors  $\mathbf{u} = (u_\ell)_{\ell=1}^d \in \mathbb{R}^d$  as follows:

$$\sigma_\ell = \phi \left( \sum_{m=1}^d h_{\ell m} u_m \right), \quad (25)$$

$$s_\ell = \sigma_\ell z_\ell, \quad (26)$$

where  $\phi$  is some nonlinear function,  $h_{\ell m}$  is a symmetric neighborhood relation, and  $z_\ell$  are mutually independent random variables. To estimate the decomposition matrix  $\mathbf{W} = [\mathbf{w}_1, \dots, \mathbf{w}_d]^\top \in \mathbb{R}^{d \times d}$ ,



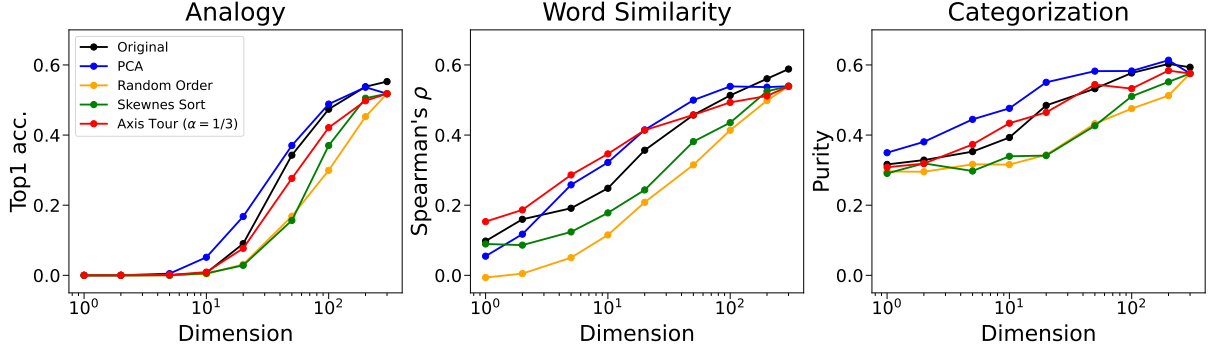


Figure 17: The performance of dimensionality reduction for the embeddings derived from word2vec. Each value represents the average of 30 analogy tasks, 8 word similarity tasks, or 6 categorization tasks.

where  $\mathbf{w}_\ell \in \mathbb{R}^d$ , such that  $\mathbf{s} = \mathbf{W}\mathbf{x}$  from the mixed signals  $\mathbf{x} \in \mathbb{R}^d$ , TICA maximize the log likelihood

$$\log L(\mathbf{W}) = \log p(\mathbf{s}, \mathbf{u} | \mathbf{W}) = \mathbb{E}_{\mathbf{x}} \left[ \log \int \prod_{\ell=1}^d \frac{p(z_\ell)p(u_\ell)}{\sigma_\ell} |\det \mathbf{W}| d\mathbf{u} \right]. \quad (27)$$

By setting  $\phi = \sqrt{\cdot}$  and applying some assumptions and approximations, the log likelihood is approximated as

$$\log \tilde{L}(\mathbf{W}) = \mathbb{E}_{\mathbf{x}} \left[ \sum_{m=1}^d G \left( \sum_{\ell=1}^d h_{\ell m} s_\ell^2 \right) \right] \quad (28)$$

where  $G$  is a function approximated by  $G(y) = -\beta_{1/2}\sqrt{y} + \beta_0$  with constant  $\beta_{1/2} = 0.8, \beta_0 = 1.2$  in our experiment. For further details on the derivation, see Hyvärinen et al. (2001a).

The optimization of (28) can be done by gradient descent:

$$\Delta \mathbf{w}_\ell \propto \mathbb{E}_{\mathbf{x}} \left[ \mathbf{x} s_\ell \sum_{m=1}^d h_{\ell m} \frac{dG}{dy} \left( \sum_{m'=1}^d h_{m m'} s_{m'}^2 \right) \right]. \quad (29)$$

Note that we have to apply orthonormalization

$$\mathbf{W} \leftarrow (\mathbf{W}\mathbf{W}^\top)^{-1/2} \mathbf{W} \quad (30)$$

to the decomposition matrix at each iteration. In accordance with the notation in (1), the extracted components  $\mathbf{S}$  are expressed by the obtained  $\mathbf{W}$  as

$$\mathbf{S} = \mathbf{X}\mathbf{W}^\top. \quad (31)$$

In summary, TICA, a kind of ICA, can extract topographic ordered features by using higher-order correlations.

## F.2 Experiments

As in classic ICA, we transform the 300-dimensional GloVe by TICA for our experiments. Following the setup of the 1-D experiment in Hyvärinen et al. (2001a), a neighborhood relation was defined by convolving a rectangular-

shaped filter  $(\dots, 0, 0, 0, \overbrace{1, 1, \dots, 1, 1}^{\text{width times}}, 0, 0, 0, \dots)$  twice with itself. Hyvärinen et al. (2001a) defined the hyperparameter width = 5 for 20 components, so for 300 components, we consider two cases where the width is scaled logarithmically or linearly to width = 9 and width = 75. These are denoted as TICA9 and TICA75, respectively<sup>22</sup>. We performed 10,000 iterations of gradient descent in both settings.

### F.2.1 Qualitative observation

Table 10 shows the examples of the axes of the TICA9-transformed embeddings and the TICA75-transformed embeddings. Similar to Axis Tour, we observe the semantic continuity of the axes in some subintervals. For example, the 250th to the 259th axes in Table 10a show the semantic continuity with respect to *countries*. Moreover, for these examples in Table 10, TICA9 seems to show the clearer semantic continuity of the axes compared to TICA75. Note that URLs, email addresses and phone numbers are anonymized in Table 10.

### F.2.2 Scatterplots of Table 10

Figures 18 and 19 show the scatterplots of the two-dimensional projections for the axes of the TICA9-transformed embeddings and the TICA75-transformed embeddings in Tables 10a and 10b.

<sup>22</sup>For the TICA9-transformed and TICA75-transformed embeddings, similar to the Axis Tour embeddings, we flip the sign of each axis as needed so that the skewness is positive.

50	51	52	53	54	55	56	57	58	59
coretta janny duncum strouse livengood	david paymer pannick costabile zdrilic	john rhys-davies naber banville koepf	betjeman john blystone bucchino newcombe	prine paulk kerrys spinnello pessoa	zuko fabricio farriss partida rionda	peter mcwhinney katis lindroos fatialofa	luís joao monteiro pereira joão	de jorge enrique josé juan	paul juan pablo mendoza scharner
100	101	102	103	104	105	106	107	108	109
sompolno družbice wartkowice dzierzgowo zanjanrud	lb4 3.7995 4-97 13/11 ,	: http://www.***.org http://www.***.com http://www.***.com www.***.com	nehzatabad poshtkuh eqbal-e zahray-ye khatunabad	anobiidae ethmia grallariidae sclerosomatidae leiothrichidae	tbur ***.com ***@***.com ***@***.com ***.com	poeciliidae dipodidae pipridae anthidium dendrobatidae	onoba sinezona anatomia cantharidus syrnola	wasbir gurubacharya tolkun aomar by	xerocomus firedred quilodran nishadham kirka
150	151	152	153	154	155	156	157	158	159
rilla vard eguchi kyeong achiou	singen referees_mike jennys regazzoni x13	bijar lali prete markazi garone	hanus goldring leura larmer similis	gò ubayy kazagham munnetra terefe	mamat myogenic ragnavd yamba swabs	boyolali gono hines strayhorn sabzevar	dammit swac ritholtz yorick elmyra	hockeyallsvenskan 94-86 86-82 second-tier	v-league lausanne-sport nasl whl divisione
200	201	202	203	204	205	206	207	208	209
two-week six-week a-half five six	35-year 50-year 60-year 25-year 40-year	epigraphic fogies old blightly gutnish	2001-2003 1998-2001 1996-1998 1999-2002 1995-1997	snags objections disagreements procedural weaknesses	sponsorship logo pitfall tagline drawcard	spectator bhb moot unfit sjc	frantic hysterical liquidator quixotic counting	appeals frivolous economized appeal 360-degree	translations translation pashto word arabic
250	251	252	253	254	255	256	257	258	259
lte ira eelam tamil fein	gam aceh milf rebel mnlf	czech poland krakow warsaw polish	russian moscow vasily sergei vladimir	anatoly ossetia ossetian oleg interfax	korean south jang korea kim	indian mukherjee bengal jharkhand bihar	serb croatia zagreb serbian croatian	romania moldova inyo iceland norway	minh nsanje chennai srinivasan chikwawa

(a) TICA9

50	51	52	53	54	55	56	57	58	59
gartenberg nart radziwill stachowski recio	faden tilles kolderie strada durrant	trescothick bopara harmse briones ruvo	.652 ramnaresh razaq taufeeq sarwan	billcliff plzen hakohen ashrafal xiangfan	dani siggins feith daugaard chedid	lentulus sivasspor najdi epps sohman	s.s.d. torrin sastra vendémiaire wenping	dakhlallah ollivier clemetson herrin sampley	matthewson feiner hatchell carrickmacross lynskey
100	101	102	103	104	105	106	107	108	109
vnccpb ustbimp gromada a_21 ***_***_****	lomartire rsst1 36.41 darreh-ye immatures	kihn apenas zgray divergens nohv	jędrzejów pleszew sokolów przysucha raciaż	cooperacion cvik hrvatske 0255 entidad	***_***_**** ohernandez .367 (928) cjones	prusice rmartinez kmorales alifereti separado	extranjero finalmente ***@***.com cantidad ***.net	:53 qe5 jgreig fedbud rx5	sa/b ***.com ***@***.com ***@***.com ***@***.com
150	151	152	153	154	155	156	157	158	159
reteamed unbeknown unbeknownst co-operate re-connect	leaf-sheaths upsmanship udalls great-grandchild nineteen	risen surged obrija soared 07:20	auguring two-song 18-yard unproduced epithalamium	i n't 've happen presume	backward-compatible satisfactorily outwardly co-existed satisfied	languishes 5.4 5.8 4.9 4.1	thursday.the one-disc 50-50 32-page hefty	expeditiously resolved sometime commence be	surged soared leapt leaped leaps
200	201	202	203	204	205	206	207	208	209
expert experts feasibility forensic study	ceremony celebrating eve parade commemorating	exams mathematics ribbon math school	vandalism campus antisocial graffiti streetscape	adjacent blocks building erected built	rocking bed sitting padded pounding	hazards investigators detect exposures remediation	recommendations advisory 301st advancement psc	27th 13th 10th 15th 23rd	cd-rom mods evolution famines experimental
250	251	252	253	254	255	256	257	258	259
titanic clot vessel tanker stotesbury	saratoga 1772 1793 thoroughbred 1794	smolensk hasselblad bonifacio cornplanter 1314	ms-dos pelts production-based conquering 1405	2g enos blandest pagan istar	pol muse plasterboard spray bmw	supermarine xk120 ground-attack turbocharged madelyn	***.com aretha banana canes amazon	ump ivf icing mapo vedanta	under-17 huon pixie southwood trikke

(b) TICA75

Table 10: Semantic continuity of axes for normalized TICA9-transformed and TICA75-transformed embeddings. For the 50th, 100th, 150th, 200th, and 250th axes, we extract ten consecutive axes from each of these axes and display the top five words for each of the extracted axes.

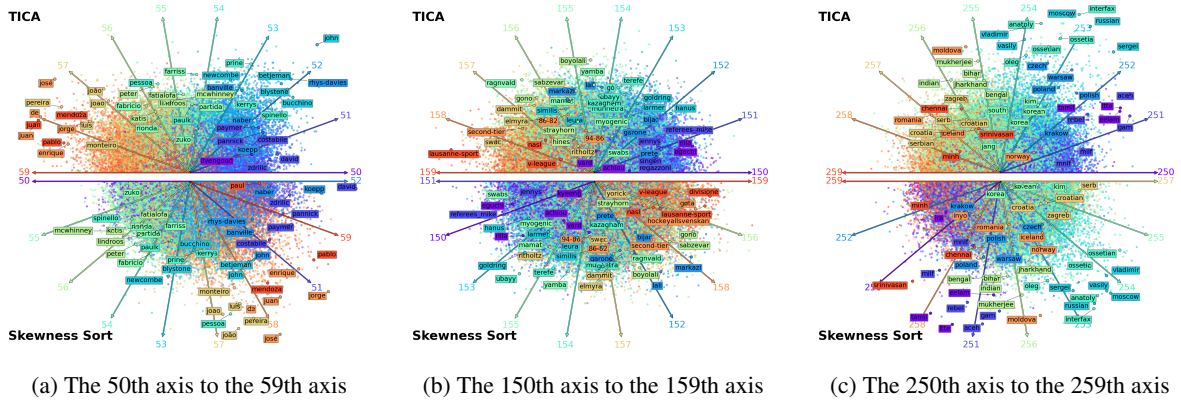


Figure 18: For TICA9, the scatterplots of the two-dimensional projections for the axes from the 50th to the 59th, from the 150th to the 159th, and from the 250th to the 259th in Table 10a.

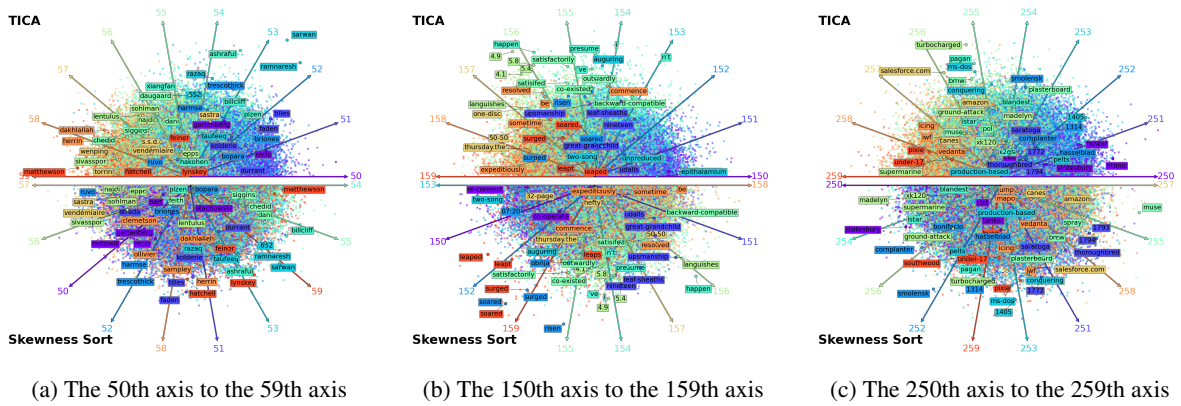


Figure 19: For TICA75, the scatterplots of the two-dimensional projections for the axes from the 50th to the 59th, from the 150th to the 159th, and from the 250th to the 259th in Table 10b.

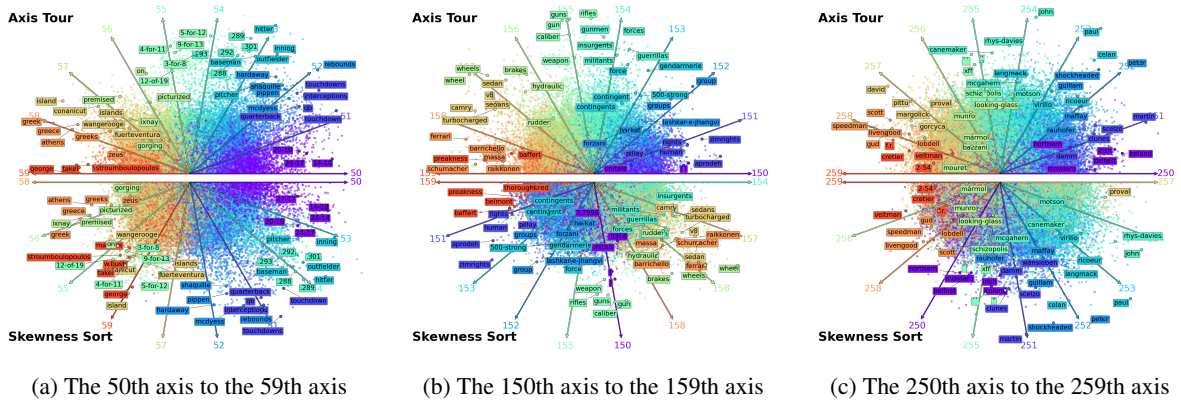


Figure 20: For Axis Tour, the scatterplots of the two-dimensional projections for the axes from the 50th to the 59th in Table 4, from the 150th to the 159th in Table 5, and from the 250th to the 259th in Table 6.

In these examples, for both TICA9 and TICA75, the interpretability of the embedding space from the scatterplots decreases as the top words of the axes show significant movement or approach the origin. This property is particularly noticeable in TICA75. For example, in Fig. 19b, the top words of the 159th axis are far from the axis: *surged* and

*soared* are concentrated near the 156th axis, and *leapt* and *leaped* are concentrated near the origin.

### F.3 Comparisons of Axis Tour and TICA

#### F.3.1 Scatterplots

This section compares the scatterplots of the TICA9-transformed embeddings in Fig. 18 and

Fig.	embeddings	$d_I$	Skew. $d_I$	diff
18a		0.61	0.59	0.02
18b	TICA9	0.33	0.35	-0.02
18c		0.57	0.54	0.03
19a		0.35	0.31	0.04
19b	TICA75	0.44	0.44	0.00
19c		0.31	0.34	-0.03
20a		0.78	0.73	0.05
20b	Axis Tour	0.72	0.58	0.14
20c		0.57	0.52	0.05
	TICA9	0.59	0.54	0.05
Avg.	TICA75	0.41	0.41	0.00
	Axis Tour	0.68	0.59	0.09

Table 11: The values of  $d_I$  for Figs. 18, 19 and 20, and the average values of  $d_I$  over 300 subintervals with  $|I| = 10$ . *Skew.* stands for Skewness Sort.

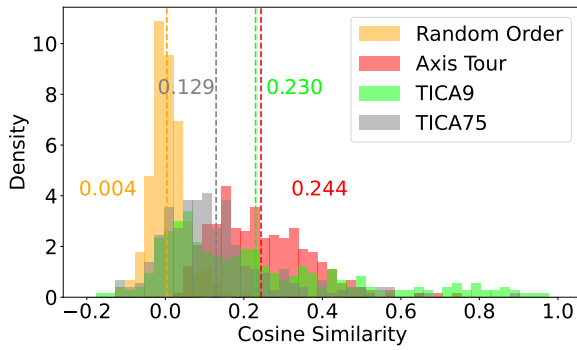


Figure 21: Histograms of cosine similarities between adjacent axis embeddings for the TICA-transformed embeddings, the Axis Tour embeddings and the Random Order embeddings.

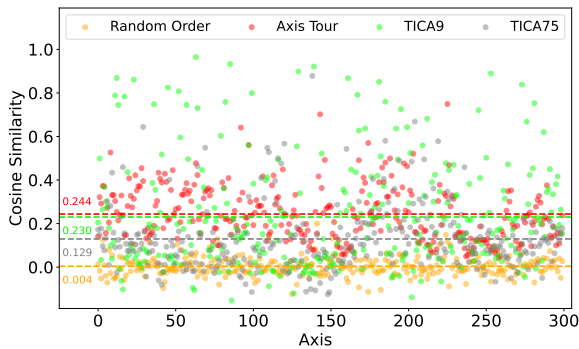


Figure 22: Scatterplots of  $\cos(\mathbf{v}_\ell, \mathbf{v}_{\ell+1})$  for Random Order, Axis Tour, TICA9 and TICA75.

the TICA75-transformed embeddings in Fig. 19 with those of Axis Tour. Since TICA9, TICA75, and Axis Tour yield different embeddings, we also compare them based on Skewness Sort.

Fig.	embeddings	$c_I$	Skew. $c_I$	diff
18a		0.35	0.21	0.14
18b	TICA9	0.09	0.03	0.06
18c		0.25	0.16	0.09
19a		0.07	0.06	0.01
19b	TICA75	0.06	0.11	-0.05
19c		0.09	0.06	0.03
20a		0.27	0.11	0.16
20b	Axis Tour	0.27	0.07	0.20
20c		0.12	0.04	0.08
	TICA9	0.23	0.14	0.09
Avg.	TICA75	0.13	0.13	0.00
	Axis Tour	0.24	0.09	0.15

Table 12: The values of  $c_I$  for Figs. 18, 19 and 20, and the average values of  $c_I$  over 300 subintervals with  $|I| = 10$ . *Skew.* stands for Skewness Sort.

First, similar to Figs. 18 and 19, we use 300-dimensional GloVe and show the scatterplots for comparison<sup>23</sup> in Fig. 20, which shows the two-dimensional projections for the axes of the Axis Tour embeddings.

Then Table 11 shows the values of  $d_I$  defined in Appendix A.3 for Figs. 18, 19, and 20, and the average values of  $d_I$  over 300 subintervals with  $|I| = 10$ . In these examples, Axis Tour shows larger  $d_I$  values and larger differences with Skewness Sort compared to TICA9 and TICA75. These results are also observed for the average values. In addition, we can see the cases where  $d_I$  is smaller than that of Skewness Sort in both TICA9 and TICA75, such as Figs. 18b and 19c.

Table 12 shows the values of  $c_I$  defined<sup>24</sup> in Appendix A.3 for Figs. 18, 19, and 20, and the average values of  $c_I$  over 300 subintervals with  $|I| = 10$ . In these examples, TICA9 shows the  $c_I$  values comparable to Axis Tour. In fact, their average values are almost the same. However, TICA9 shows larger  $c_I$  values even when Skewness Sort is performed on  $I$ . This suggests that for the TICA-transformed embeddings, the axes with similar meanings tend to cluster locally rather than being ordered so that the meanings are continuous. This hypothesis could

<sup>23</sup>Note that Figs. 1 and 6 show the scatterplots for the illustrative examples, so it is unfair to compare them directly with those of TICA.

<sup>24</sup>For the TICA9- and TICA75-transformed embeddings, as with Axis Tour embeddings,  $c_I$  can be computed by the cosine similarities of adjacent axis embeddings.

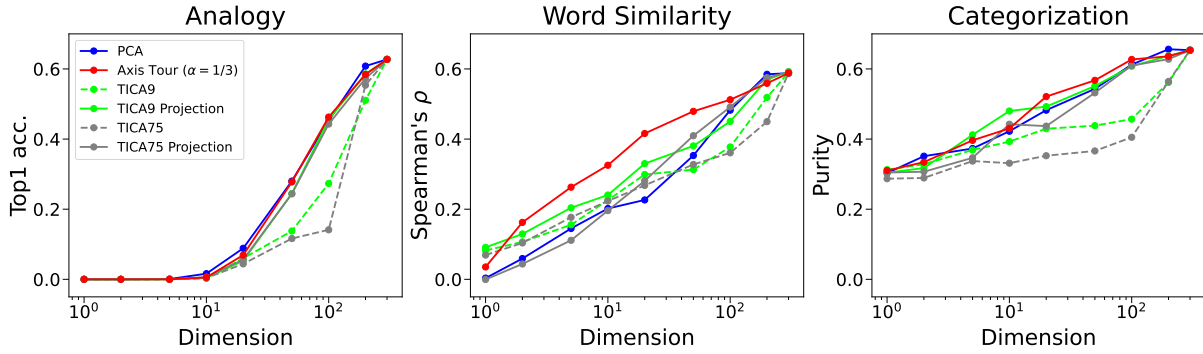


Figure 23: The performance of dimensionality reduction for the PCA-transformed embeddings, the Axis Tour embeddings with  $\alpha = 1/3$ , the TICA-transformed embeddings, and the TICA Projection embeddings with  $\alpha = 1/3$ . Each value represents the average of 30 analogy tasks, 8 word similarity tasks, or 6 categorization tasks.

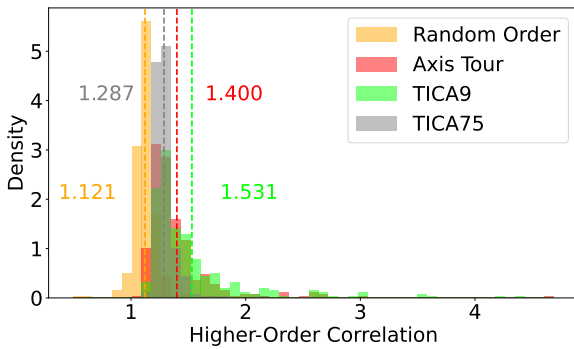


Figure 24: Histograms of higher-order correlations between adjacent axes for the TICA-transformed embeddings, the Axis Tour embeddings, and the Random Order embeddings.

explain why, in the scatterplots such as Figs. 18 and 19, the top words of the axes show significant movement or approach the origin.

In TICA75, the  $c_I$  values are lower, and the difference in the average value compared to Skewness Sort is 0. This indicates that the axes with less similar meanings are grouped together in  $I$ , resulting in no difference in  $c_I$  between TICA and Skewness Sort.

### F.3.2 Cosine similarity and higher-order correlation

Figure 21 shows the histograms of  $\cos(\mathbf{v}_\ell, \mathbf{v}_{\ell+1})$  of the TICA-transformed embeddings, the Axis Tour embeddings and the Random Order embeddings. Similar to Axis Tour, The distribution for TICA shifts towards a more positive mean than that of Random Order. Note that while TICA9 has an average close to that of Axis Tour, it has a significantly higher variance of cosine similarity.

To highlight this, Fig. 22 shows scatterplots of cosine similarities between adjacent axis embed-

dings. The variance is 0.05 for Random Order, 0.12 for Axis Tour, 0.25 for TICA9, and 0.15 for TICA75. The variance for TICA9 is significantly larger than that for Axis Tour, which indicates that the semantic continuity of the axes changes more drastically in the TICA9-transformed embeddings.

Figure 24 shows the histograms of higher-order correlations between adjacent axes of the TICA-transformed embeddings, the Axis Tour embeddings and the Random Order embeddings. We can see that the average higher-order correlation for TICA is higher than that for Axis Tour, reflecting the learning settings of TICA.

### F.3.3 Dimensionality reduction: analogy, word similarity, and categorization tasks

This section performs dimensionality reduction for TICA, selecting the axes sequentially starting from the first, similar to Random Order and Skewness Sort.

As we saw in Appendix E.4, we defined Random Order Projection and Skewness Sort Projection by the dimensionality reduction process similar to that of Axis Tour. A similar approach can be considered for TICA, and we call this method TICA projection.

Figure 23 shows the average of each task at  $p = 1, 2, 5, 10, 20, 50, 100, 200, 300$  for the Axis Tour embeddings, and TICA-transformed embeddings. Axis Tour outperformed both TICA and TICA Projection for most dimensions in each task. Note that similar to the results for Random Order and Skewness Sort in Appendix E.4, TICA Projection shows performance improvements over TICA in most dimensions. These results demonstrate the utility of projection-based dimensionality reduction even in TICA, an algorithm that relaxes the

Role	Prompt
system	You are an excellent NLP annotator. Your response should be in JSON format with the key 'choice'.
user	Which of the following words are related to the words [ <i>top1 word</i> , . . . , <i>top10 word</i> ]. Answer A or B. A. [ <i>Axis Tour top1 word</i> , . . . , <i>Axis Tour top10 word</i> ] B. [ <i>Skewness Sort top1 word</i> , . . . , <i>Skewness Sort top10 word</i> ]

Table 13: Prompts for the GPT models. Since the Axis Tour embeddings and the Skewness Sort embeddings differ solely in the order of the axes, they share  $d (= 300)$  common axes. The top 10 words for each common axis are denoted as [*top1 word*, . . . , *top10 word*]. We focus on the next axis of Axis Tour and the next axis of Skewness Sort, based on the common axis. The top 10 words for the Axis Tour axis are denoted as [*Axis Tour top1 word*, . . . , *Axis Tour top10 word*], while the top 10 words for the Skewness Sort axis are denoted as [*Skewness Sort top1 word*, . . . , *Skewness Sort top10 word*]. We then use the top words for the prompt.

Model	Version
GPT-3.5 Turbo	gpt-3.5-turbo-0125
GPT-4 Turbo	gpt-4-turbo-2024-04-09
GPT-4o	gpt-4o-2024-05-13
GPT-4o mini	gpt-4o-mini-2024-07-18

Table 14: Version of each GPT model.

assumption of statistical independence for ICA.

## G Details of the quantitative evaluation of semantic continuity by GPT models

This section provides details on the GPT models, accessed via the OpenAI API, and the prompts used in Section 5.2.2.

The versions of the GPT models used in the experiments are listed in Table 14. The prompts used for the experiments are shown in Table 13. In Fig. 3, the responses obtained from each model using these prompts are aggregated and shown. Note that GPT-4 Turbo failed to provide responses relevant to either Axis Tour or Skewness Sort for two queries.